uc3m | Universidad Carlos III de Madrid

Bachaelor's Degree in Biomedical Engineering

Academic Year (2018-2019)

Bachelor Thesis

"Dissolved oxygen determination in two-dimensional tissue cultures using optical sensors"

Cristina López Serrano

Nuria López Ruiz

Leganés, Junio 2019

ABSTRACT

Oxygen concentration determination is of importance across many different industries, biomedical research among them. In biological systems, in vivo oxygen levels vary across a wide spectrum and strongly influence function of cells and tissues. Direct measurements of oxygen tension and its progression in real-time are necessary in order to understand and control cell survival, proliferation and differentation. In this thesis, special attention is payed to skin tissue. An in-depth understanding of these aspects will allow to provide better diagnostic and therapeutic tools for wound care.

The general objective of this thesis is to analyze dissolved oxygen concentration in a two-dimensional tissue culture of a keratinocyte cell line (HaCaT) via the development and application to this purpose of an optical sensor. The sensor is based on a metalloporphyrin membrane (PtOEP) that emits a fluorescence signal that is quenched by oxygen in the environment. Images of the membrane are captured using time-lapse microscopy with a filter at the desired wavelength. Average pixel value is then analyzed, as it is directly related to O_2 concentration.

The porphyrin-based optical sensor developed in this work is proved to be compatible with cell culture. Using this sensor, changes in oxygen concentration in a physiological range can be detected. Dissolved O_2 concentration in culture medium is found to decrease at high cell densities as a result of O_2 consumption. It is also possible monitor discontinuities in a monolayer of cells by detection of local O_2 concentration using this sensor.

Keywords: Optical sensors, oxygen sensors, photoluminescence, metalloporphyrin

ACKNOWLEDGEMENTS

Cuando era pequeña quería ser científica, de esas con bata blanca que mezclaban liquiditos de colores en tubos de ensayo. Ahora que sé un poco más de lo que conlleva, creo que mi yo de 11 años estaría contenta si me hubiera visto trabajando en este proyecto. Quiero dar las gracias a todas las personas que han estado en mi camino y me han ayudado a llegar hasta aquí.

A Nuria y a Dahiana, por darme esta oportunidad, por dar ánimos y nuevas ideas cuando parecía que nada salía bien.

A los técnicos del laboratorio de bioingeniería, por abrirme siempre la puerta con una sonrisa, incluso cuando era la quinta vez que llamaba en el mismo día.

A la gente de CEEIBIS, por enseñarme un mundo universitario más allá de las clases.

A mis amigos. A las de la uni, porque este camino sin vosotras hubiera sido, como mínimo, más aburrido. A los de Purdue, por hacer que ese año vaya ser inolvidable. A Ceci, por escucharme siempre, por sacarme de paseo cuando me dejo sacar.

A mi familia, en especial a mis padres, por estar ahí siempre. A mi madre, por su sentido práctico, por ser los ojos que me aportan una perspectiva nueva.

CONTENTS

LIST OF FIGURES

LIST OF TABLES

1. INTRODUCTION

1.1. Motivation

Cell culture remains as one of the most used methods to study cell behavior and experiment *in vitro*. An in-depth understanding of the environmental characteristics that affect these cells, such as temperature, pH, gas composition or pressure, is therefore necessary in order to explain and control their function. Oxygen concentration is one of such parameters that has been shown to profoundly affect the cells.

Cells in the body respond to different oxygen levels depending on the tissue they reside in and this can influence their function. For example, gradients of oxygen in the liver are thought to be the main factors in zonal variations of hepatocyte activity [1]. Also, angiogenesis, tissue repair and tumor growth are dependent on oxygen levels and the expression of oxygen responsive genes [2]. For the case of skin cells, hypoxia is a crucial physiological signal that marks the onset of wound healing, although long-term low O_2 levels are not desirable as they lead to a decreasing cellular response [3] and can favor bacterial proliferation.

Emerging 3D culture technologies, such as tissue-on-a-chip devices, call for a study of oxygen diffusion through three-dimensional tissues. In traditional 2D cultures, oxygen and nutrients are readily available for the cells from culture media. However, these conditions differ in 3D cultures, as diffusion has to take place. Mathematical models that explain this process have been developed [4] but studies that show experimentally this behavior *in vitro* are still necessary.

As a result, direct measurements of oxygen tension and its progression in real-time are necessary in order to understand and control cell survival, proliferation and differentiation. Specifically speaking about cell culture, dissolved oxygen concentration in culture media is an important factor to take into account. Current oxygen sensing systems, such as the Clark electrode, are not always suitable for this application, as they can lead to contamination of the cells or are not usable for long-term monitoring. Optical oxygen sensors provide a non-invasive method to determine oxygen levels. This work aims to

apply an optical oxygen-sensing method to skin cell cultures to study O_2 diffusion in 2D. It will also set the bases for future work regarding O_2 diffusion in 3D tissues *in vitro*.

1.2. Objectives

The general objective of this thesis is to analyze dissolved oxygen concentration in a two-dimensional tissue culture via the development and application to this purpose of an optical sensor. The specific goals that lead to the final aim are:

- To characterize the optical sensor and optimize of the fabrication protocol.
- To measure experimentally oxygen variations in 2D cellular cultures and to establish a relation between oxygen concentration and presence of cells at different densities.
- To develop a basis for oxygen diffusion studies in 3D cellular cultures.

1.3. Project Planning and structure of the document

The project described in this document was developed from November 2018 to May 2019. The work was structured in five main phases along those months, as shown in figure 1.1:

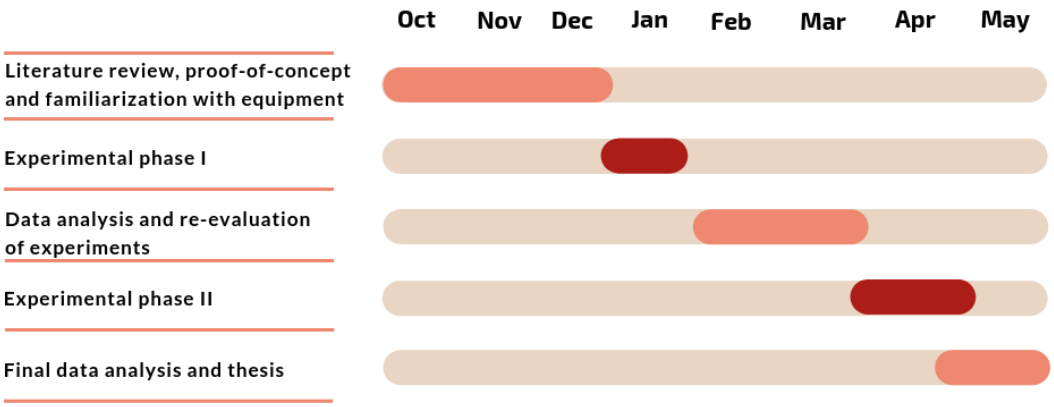

Fig. 1.1. Gantt Diagram

- **Phase I** *(Oct-Dec 2018)*: Literature review, proof of concept and familiarization with equipment

This initial phase involved reading documentation concerning the subject in order to learn the main concepts and state-of-the-art. A preliminary experiment had already been carried out in June before deciding the beginning of this project. This experiment was repeated during these months in order to demonstrate the feasibility of this work and determine the main problems and improvement areas with the technique. These months also served to familiarize with the equipment to be used, namely the fluorescence microscope.

- **Phase II** *(Jan 2019)*: First experimental phase
  Experiments to characterize the sensor were carried out, then first oxygen level measurements were performed.

- **Phase III** *(Feb-Mar 2019)*: Data analysis and re-evaluation of experiments
  The data acquired in the previous phase was analyzed and, taking into account the results, the steps of the project were re-evaluated to account for the problems that had appeared.

- **Phase IV** *(Mar-Apr 2019)* Second experimental phase
  The second round of experiments was performed. This phase involved more specific experiments targeting more specific objectives regarding O_2 diffusion measurements.

- **Phase V** *(May 2019)*: Final data analysis and thesis
  Once all the necessary data had been acquired, it was analyzed and the present thesis was written.

This document collects all the information regarding this project. The first chapter puts the work in context and general information is described. The body of the work is divided in three main sections. Chapter 2 explains the state-of-the-art, background on cell culture and oxygen monitoring. Chapter 3 includes a description of the materials and methods employed, intended to detail all the processes involved. The fourth chapter presents the results obtained and shows the analysis and the conclusion drawn from them. The fifth chapter explains the conclusions and future lines of work. Finally, the last chapter aims to present the economic and regulatory framework of the project as well as the budget.

2. BACKGROUND AND STATE OF THE ART

In this chapter, the theoretical background concepts necessary for the development of this work will be described.

2.1. Basic concepts on cell culture. Skin and wound healing

2.1.1. Overview of cell culture concepts

Cell culture of immortalized cell lines

New techniques for biological studies are rapidly emerging nowadays, such as the use of high throughput computational modelling or microfluidic devices. Despite these advances, traditional cell culture remains as the first step for *in vitro* studies of most current research. This thesis is focused on the development of an oxygen sensor for such applications. To achieve this purpose, it is first necessary to understand some of the basic concepts regarding cell behavior and cell culture.

Immortalized cell lines are cells that have been artificially manipulated to proliferate indefinitely. They provide several advantages as opposed to primary cells: they are very well characterized, provide genetically identical populations and grow more robustly. They also eliminate the ethical issues related to the extraction of cells from a living being. The major disadvantage is that these cells might express some unique gene patterns and not have relevant attributes or functions of normal cells [5]. Considering the needs of the projects, an immortalized line is the choice for the cellular studies.

Cell culture conditions

Culture medium is a crucial aspect of the cell culture environment, as it provides the necessary nutrients, hormones and growth factors, as well as regulating the pH and osmotic pressure [6]. Phenol red is a common ingredient of culture medium, as it serves as a visual indicator of pH. Since the activity of the sensor developed in this project involves red fluorescence, medium without phenol red is used during the experiments to avoid any potential interference on measurements.

Most normal mammalian cell lines growth at pH 7.4. To enhance cell survival and proliferation, cells are maintained in an incubator at 37°C, with 5% CO_2 in air. Since normal air oxygen concentration is around 21%, the incubator atmosphere with added CO_2 will provide an oxygen concentration of 19,95%.

Confluency and cell proliferation

Confluency is a concept repeated along this thesis, referring to the density at which the cells are seeded in culture (e.g. 80% confluency means 80% of the surface of the culture plate is occupied by cells). This is calculated by multiplying the number of cells by their theoretical surface area and dividing that number by the area of the culture dish. A confluent monolayer refers to cells that form a cohesive sheet that occupies the entire culture surface.

Proliferation is the increase in number of cells due to their division and is regulated by growth factors that induce cells to enter in the cell cycle. Immortalized cells, such as the ones used in this project, have a high proliferation rate. It is a key marker of cellular activity and crucial for aspects such as tissue regeneration. There are several methods to measure cell proliferation, most of which are based on measurements of some marker of metabolic or enzymatic activity [7]. For this thesis, a commercial kit of alamarBlue® is used, which is based on a cell permeable redox indicator, resazurin. "Viable cells with active metabolism can reduce resazurin into the resorufin product, which is pink and fluorescent" [7]. Figure 2.1 shows the molecular structure of resazurin and the reaction it undergoes to form the fluorescent resorufin product.

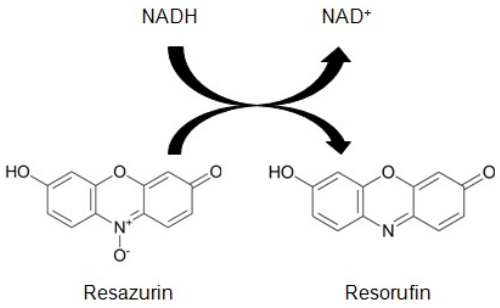

Fig. 2.1. Structure of resazurin and resorufin products [7]

Culture substrate

Adherent cells require a surface to attach to and grow on, where they organize in a two-dimensional sheet. Generally, polystyrene petri dishes are used for cell culture. The

sensor described in this study consists of a thin film with a fluorophore that is placed under the cells. In order to obtain an appropriate surface for cell culture, a layer of polydimethylsiloxane (PDMS) is placed on top of it. PDMS is chosen thanks to its desirable properties: chemical inertness, thermal stability, gas permeability, low cost, ease of manipulation [8] and optical transparency. However, its intrinsic hydrophobicity is the main factor that results in poor cell adhesion, creating clusters of cell aggregates that dissociate [9]. There are several strategies to address this issue. Some studies explore oxygen plasma treatment as a way to reduce hydrophobicity of PDMS surfaces [10]. The method of choice in this study is to use an extracellular matrix protein, collagen, as coating.

2.1.2. Skin cells. Wound healing

Skin is the largest organ of the body, covering an area of about $2m^2$ in adults. It is composed of two main parts: the superficial epidermis and the deeper, thicker dermis (Fig. 2.2). The epidermis is composed of keratinized stratified squamous epithelium. It is mainly formed by keratinocytes, which are organized in four or five layers. The dermis is composed of dense irregular connective tissue containing collagen and elastic fibers [11]. Skin is of great interest for pharmaceutical and cosmetic companies, as it is in direct contact with topically delivered drugs, cosmetics, pathogens, etc. It is also a relatively simple organ regarding its structure.

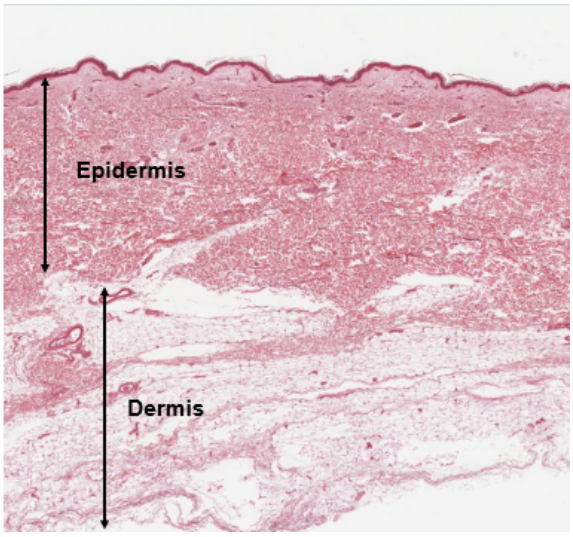

Fig. 2.2. Skin histological slide. *Source: Image adapted from Michigan's collection of virtual microscope slides & slides for Junqueira's basic histology. Indiana University[12]*

Cells used in this project are a keratinocyte cell line, HaCaT. Keratinocytes have a rounded shape, with a diameter of about 20-25μm. They are an important component of wound healing and also involved in inflammation. In the body, keratinocytes are assembled in layers. For this project, a monolayer of keratinocytes will be used. Fig. 2.3 shows a microscopic image of the cells used for the project.

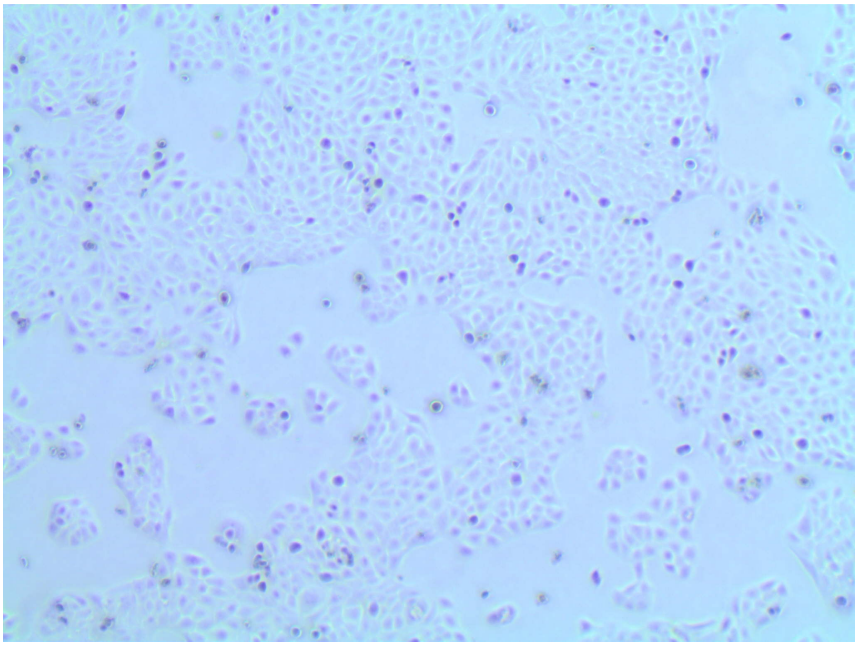

Fig. 2.3. Microscopic image of HaCat cells

2.2. Dissolved oxygen determination

2.2.1. Importance of oxygen levels

A major challenge for the development of more complex cell culture system is the delivery of nutrients and other necessary molecules, such as oxygen. Oxygen presents slower diffusion and higher consumption compared to other major nutrients, which limits oxygen transport *in vitro* [3]. However, presence of oxygen is not only crucial for cell survival, but oxygen levels also affect and modulate cell function.

Local oxygen concentration has role in cell differentiation. Holzwarth et. al. [13] showed that reduced oxygen tension severely impaired adipogenic and osteogenic differentiation of human mesenchymal stem cells. Bassett and Hermann [14] found that embryonic stem cells differentiate towards the bone lineage when in hyperoxic conditions (35% O_2),

while cartilage cells were formed under hypoxia (5% O_2).

Differences in oxygen concentration in physiological systems provide key signals for specific cell functions. A relevant example of this is liver zonation. The physiologically occurring gradient of oxygen in this organ is considered to be necessary to allow the various metabolic pathways to run in parallel in the most efficient manner [15]. This is achieved thanks to different localizations of vasculature, that provide higher or lower oxygenation.

Oxygen concentration is also a key factor for in vivo wound healing. O_2 consumption has been demonstrated to be a relevant parameter in local treatment of damaged tissue [16]. The revascularization of wounds is a crucial step for healing. Studies show that the center of wounds remains low in oxygen and that this hypoxic gradient disappears when the new blood vessels have completely grown across the wound [17]. "This wound induced acute hypoxia is believed to be an important signal during all phases of wound healing because it regulates cell proliferation, migration and differentiation through the induction of cytokines and diverse intracellular signalling pathways" [3]. Regarding keratinocytes, motility of these cells is increased under low oxygen conditions, which results in favorable re-epithelialization [18]. As a result, occlusive wound dressings promote early skin regeneration. Although acute local hypoxia in the micro-environment of the wound facilitates healing, chronic hypoxia caused by inadequate vascularization decreases cellular wound healing responses. With that in mind, hyperbaric oxygen therapy is a common treatment for patients with chronic wounds.

"Ultimately, environmental oxygen differences between tissue culture and in vivo physiology can hinder translating research findings from benchtop to bedside. Studying cells in inaccurate environments makes predicting appropriate drug dosages for in vivo models difficult, leading to drug failure during clinical trials" [19]. Therefore, it appears necessary to develop a method to closely monitor oxygen tension in cell culture that allows research in disease and drug development to efficiently simulate physiological conditions for *in vitro* studies.

2.2.2. Experimental methods for oxygen determination

Determination of oxygen concentration in the gas phase or dissolved in a liquid is highly demanded for many applications. An increasing concern over environmental pollution and public health issues has called efforts to develop accurate real-time measurements of gases. It is similarly essential for the food industry, especially in food packaging. Finally, in the biomedical field, very precise oxygen determination is needed for cell culture, treatment and diagnosis. As a result, different types of oxygen sensors have been developed. Some examples are explained below.

Winkler titration

This method has been largely employed to determine oxygen concentration in water, and is to some extent considered standard. It consists of adding an excess of manganese (II) salt, sodium iodide and sodium hydroxide to water. Dissolved oxygen will oxidize the precipitate. Next the solution is acidified by HCl [20], allowing to calculate the amount of dissolved oxygen via this titration. Despite the simplicity of this technique, it has been widely substituted by newer technological solutions, as extremely careful and time-consuming manipulation is necessary.

Clark oxygen electrode

The development of the Clark electrode in 1953 [21] provided a revolutionary technique that has become the conventional method. It consists of a platinum cathode and a silver anode immersed in a saline solution (KCl) (Fig. 2.4). Oxygen reduction takes place at the cathode when the power supply applies a potential. The current of the reduction of oxygen, which is proportional to oxygen concentration, is recorded [22].

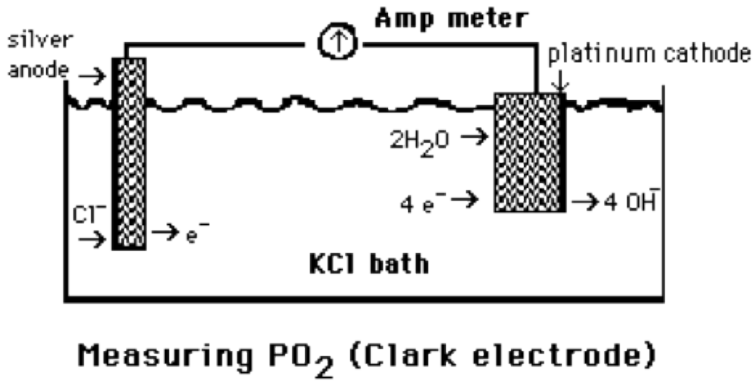

Fig. 2.4. Clark electrode[23]

Despite the widespread use of Clark electrodes, they suffer from some significant limitations [22]:

- Response time is limited by the time taken for diffusion of O_2 through the membrane.
- Cross-sensitivity of non-targeted gases may result in false readings.
- The electrodes consume oxygen, therefore potentially generating misleading data.
- Difficult miniaturization. Electrodes are too large to be used in microvasculature, and disrupt circulation, altering measurement conditions.

These drawbacks justify the interest on optical solutions, together with the advantages that these kind of sensors can provide, such as being non-invasive.

2.2.3. Optical detection of oxygen

Optical sensors are cheap, easy to miniaturize, specific and do not suffer from electrical interference. They are based on materials that change their properties in presence of gaseous or dissolved oxygen, generally absorption or luminescence [24]. The use of an optical sensor depends mainly on the method of determination and the optical sensing probe.

Absorption-based sensors

Changes in color observed by eye can offer qualitative or semi-quantitative information while changes in absorbance or reflectance allows to obtain quantitative values by means of a external detection unit [24]. Different molecules and chemical properties are taken advantage of for this purpose:

- Oxygen carriers that have different absorbance when oxygenated versus deoxygenated. An example is hemoglobin, used for common pulsoxymetry [25].
- Redox systems or light-driven redox reactions. Nanoparticles of titanium can be used to photosensitize the reduction of methylene blue, resulting in its bleaching upon UV irradiation. The indicator remains in this colorless state in the dark until it is exposed to oxygen, when it recovers its original color [25].

Luminescence-based sensors

Most optical oxygen sensors are of this type, based on quenching of luminescence dyes by oxygen. "As oxygen quenches both the luminescence intensity and excited-state lifetime, there are inherently two different methods of measuring oxygen concentrations or pressures with luminescent probes" [26]. Intensity based sensors are easier to implement, as they just concern detection of fluorescence intensity over a period of time. Despite this, some research is focused on the development of life-time based sensors, as they provide more robust measurements, better contrast and suppression of background signal [26]. The sensor used in this project is intensity-based.

Some examples of optical sensing probes used for oxygen detection, as described by Wang et al. [27], are:

- *Organic luminescent probes*: Pyrene and its derivatives have relatively long excited-state lifetimes and are efficiently quenched by oxygen, so they have been selected as fluorescent probes.

- *Metal-complex organic dyes*: They present strong luminescent intensity and long life-times. They are two main types: transition metals and metalloporphyrins. Ru(II) polypyridyl, the most frequently used transition metal complex, has a fluorescence which is dominated by the metal-to-ligand charge transfer process. Metal porphyrins, specifically Pd and Pt, are the most efficient luminophores. Since this project deals with a Pt-porphyrin complex, they will be explained in detail in the following subsection.

- *Dual emitters*: They make use two largely different emission bands, one with a decay time in the nanosecond range that is insensitive to oxygen (reference band), being the second a long-lived highly-sensitive oxygen-quenchable emission. This way, the ratio between the two signals is calculated as a measure of O_2 concentration.

- *Luminescent nanocrystalls*: especially quantum dots, present intense brigthness and high photostability. However, only few of them present reversible excitation to oxygen.

2.2.4. Porphyrin complex

Porphyrins are a class of macrocyclic aromatic compounds composed of four pyrrole rings connected by methine bridges [28]. These molecules naturally combine with metals to form metalloporphyrins. The porphyrin nucleus is a tetradentate ligand in which the space available for a coordinated metal has a maximum diameter of 3,7Å[29]. The most widely known one is heme, which contains an iron ion in the middle and is a component of hemoglobin. Variations of this structure with different attached metals provide many technical applications. Nardis et al. [30] report preparation of a cobalt-porphyrin thin film that shows a fast and reversible response towards the detection of methanol vapors. The same complex is used by Delmarre et al. [31] grafted in a sol-gel matrix for amine detection. Another example is an Indium-porphyrin complex used for determination of chloride in human serum samples [29]. For this project, a platinum octaethylporphyrin complex (PtOEP) (Fig. 2.5) is used.

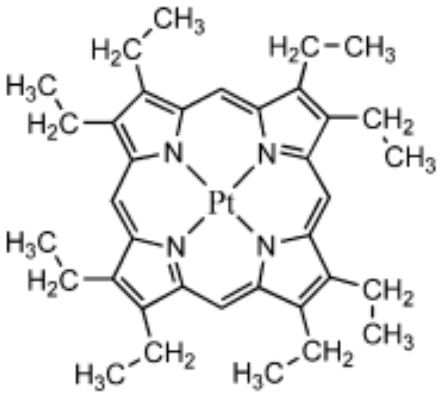

Fig. 2.5. Platinum octaethylporphyrin molecule [27]

Upon platinum complexation, porphyrins exhibit fluorescence prone to dynamic quenching by oxygen, which allows films made with this molecule to be used for oxygen sensing. The general idea of the sensing procedure is that, when irradiated at the excitation wavelength, the films will emit a fluorescence signal that is affected by environmental oxygen level (higher levels of oxygen result in lower emission intensity). “Among all oxygen probes, Pt and Pd porphyrin complexes are the most efficient luminophores, since they present strong luminescence at room temperature, absorb visible light and show large Stokes shifts about 200 nm” [27]. These characteristics make PtOEP an ideal candidate

for oxygen sensing purposes. In figure 2.6 the excitation and emission spectra of PtOEP are shown. It is observed that maximum excitation occurs at 383nm and 535nm. Although the higher peak corresponds to the former, that wavelength lies in the ultraviolet region and is harmful for cells. Therefore, for the purpose of oxygen sensing of cell culture excitation at 535nm (green) is desired. With respect to fluorescent emission, the peak is at 645nm (red) regardless of the excitation wavelength.

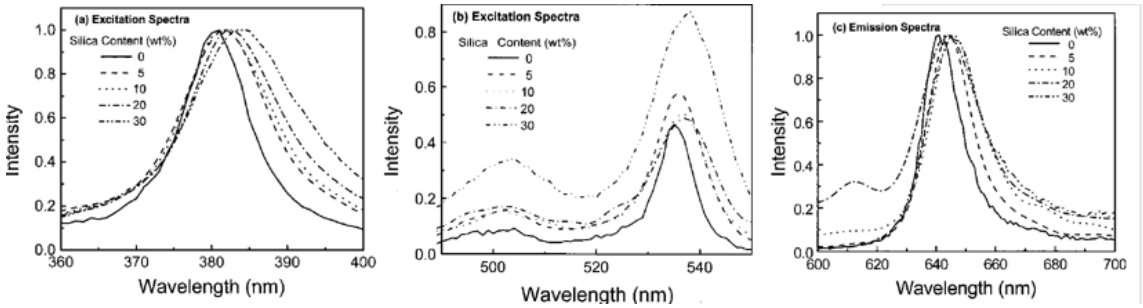

Fig. 2.6. PtOEP emission and excitation spectra [32]

Several uses of metalloporphyrins in oxygen sensors have already been reported in literature. An interesting example is reported by Ricketts et al. [33]. A sensor with a "traffic light" (red-yellow-green) response is developed using PtOEP incorporated in an ethyl film and a green led, used both as an emitter and excitation source for the porphyrin complex (set up shown in Fig.2.7). At high O_2 partial pressures emission from PtOEP is quenched and the light from the green led is the prominent colour, as O_2 partial pressure increases, the luminophore film is not quenched and red becomes the dominant colour.

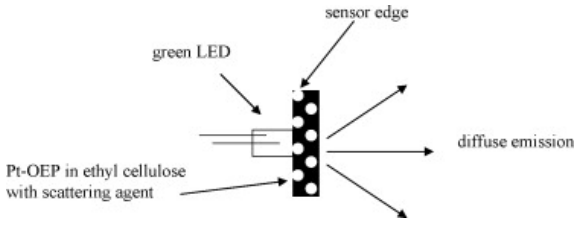

Fig. 2.7. "Traffic-light" sensor by Ricketts et al. Schematic of the sensor design [33]

Bhagwat et al. [34] used a thin film of a porphyrin complex immobilized in PDMS, similar to the one used in this project, and proved that images acquired with a colour camera display red fluorescence (645nm) which is directly related to the concentration of oxygen. The excitation wavelength used is 390nm, which provides optimal response, that can be seen by eye as shown in Fig. 2.8.

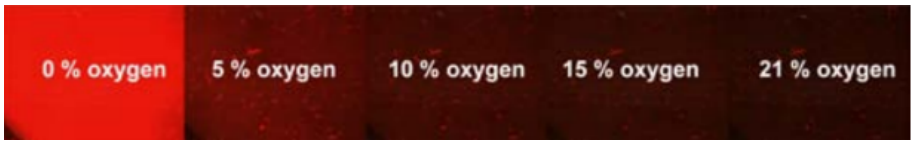

Fig. 2.8. Colorimetric sensor by Bhagwat et al. [34]

In addition, some authors have already developed research on the application of these porphyrin-based oxygen sensors to biological studies, specifically *in vitro* cell culture. Rivera et al. [19] use an integrated phosphorescence based photonic sensor, in this case based on a palladium-benzoporphyrin derivative embedded in a hydrogel, to monitor oxygen levels in breast epithelial cell culture.

The article "A Noninvasive Thin Film Sensor for Monitoring Oxygen Tension during *in vitro* Cell Culture", by Thomas et al. [35], has been an important reference for this project. They report preparation of an oxygen sensor based on two different assemblies of a platinum-porphyrin complex (PtTFPP), Fig.2.9A. They force step changes of O_2 concentration and study oxygen consumption by cells. From the graph in Fig. 2.9B, they conclude that, at high cell densities, there is a significant decrease in the local oxygen concentration, as the consumption cannot be compensated by diffusion from the environment.

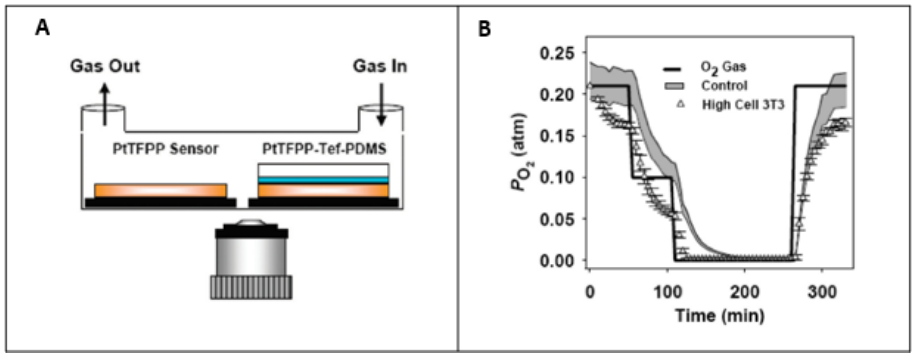

Fig. 2.9. *In vitro* oxygen sensor by Thomas et al. [35]. A: Experimental setup. B: Oxygen measurements in the presence of high cell density

Another example is the Pt-porphyrin-based hydrogel fabricated by Zeng et al. [36]. In this case, the sensor is able to provide real time oxygen measurements in a culture of human cervical cancer cells.

2.2.5. Further advances: optical fiber sensors and in vivo measurements

Research is already progressing to turn the thin film sensors into more flexible formats, that allow easier miniaturization and more accurate measurements. A line of investigation is the development of optical fiber sensors, that allow a highly localized excitation and an improved signal to noise ratio. Pulido et al. [37] managed to immobilize a Ruthenium luminophore on a commercial polymer optical fiber, using an easy and reproducible method for oxygen sensing. The use of optical fibers is considered of interest for the long-term goal in which this thesis is framed, as they would allow to obtain information about oxygen concentration at different layers of a 3D culture, and therefore study O_2 diffusion.

Regarding in vivo experimentation, the application of optical detection technologies allows to provide quantitative measurements of dissolved oxygen concentration in situ, using miniaturized, minimally invasive devices. This is specifically of interest for the study of microvasculature, since common electrodes can disrupt or block blood flow in small vessels. Vinogradov et al. [38] used this technique to visualize oxygen concentration in tumor-bearing mice. To do so, they injected they luminophore in the circulation, and imaged the animals using the appropriate wavelength (Fig. 2.10). They claim that increased phosphorescence is seen at the tumor site due to a combination of higher blood flow and lower oxygen partial pressure. Sinaasapel et al. [39] studied the use of a palladium-porphyrin sensor in vivo, coupling the dye to albumin in order to restrict it to the circulation and to measure oxygen in the physiological range.

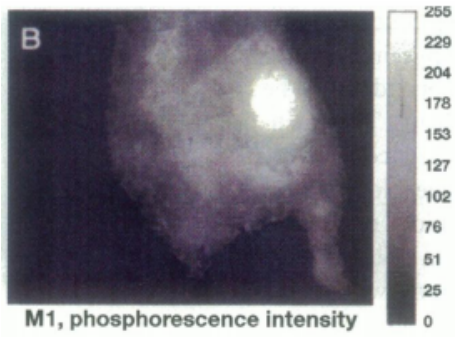

Fig. 2.10. In vivo oxygen sensor by Vinogradov et al. [38]. Increased fluorescence is seen at the tumor site.

Another example of in vivo measurements is reported by Meier et al. [40]. In their

article, they describe a polymeric matrix which is integrated with two luminophores, responsive to O_2 concentration and pH respectively. After thorough characterization, they apply the sensor on healthy and damaged tissue and, following excitation of the membrane at a specific wavelength, they are able to obtain measurements of pH and O_2 concentration *in situ*. These measurements serve to understand cell behavior during wound healing and to better design dressings and treatments which adapt to the needs of the tissue.

2.3. Theoretical oxygen delivery and measurements in 3D tissue

While it is indeed interesting to determine oxygen concentration in 2D tissue cultures, it becomes of special relevance when considering 3D structures, since not all the cells are in direct contact with the environment and delivery has to be considered, to avoid hypoxic or anoxic regions. Specifically for the example of 3D skin tissue, Matellán [4] derived the equations and built a mathematical model to explain oxygen delivery. For simplicity, the model considers two layers of skin, epidermis and dermis, and two oxygen sources, the outer environment and inner delivery from microchannels (analogous to capillaries). Figure 2.11 displays the oxygen concentration profile for a thin layer of skin. Further development of minimally invasive optical sensors for *in vitro* culture will allow to experimentally prove this theoretical model.

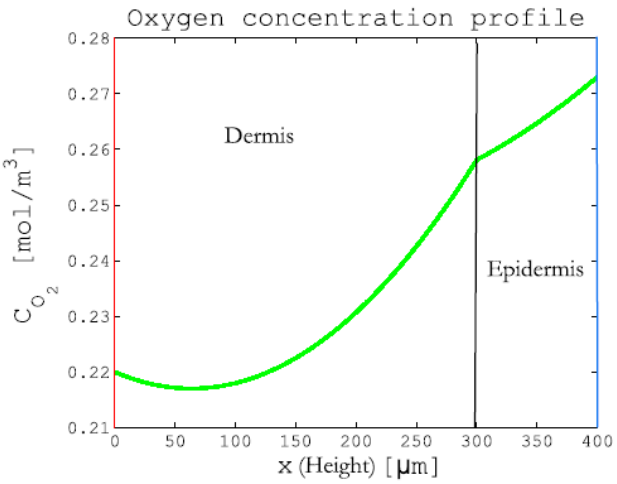

Fig. 2.11. Mathematical model for oxygen concentration profile in the dermis and epidermis [4]

Some authors have already applied porphyrin-based optical sensors to monitor oxygen concentration in three-dimensional tissues. Weyand et al. [41] use phosphorescent micro-

beads as a noninvasive method to determine oxygen concentration in 3D tissue cultures inside a bioreactor. Rivera et al. [19] designed an integrated phosphorescence-based oxygen biosensor (iPOB), which was used to measure differences in oxygen environment between tumorous and healthy tissues of breast epithelial cells seeded three-dimensionally in Matrigel®. Similarly, Zirath et al. [42] use a PDMS chip with four sensing spots to monitor oxygen concentration in a fibrin hydrogel seeded with human umbilical vein endothelial cells (HUVEC).

2.4. Theoretical concepts for fluorescence imaging

In this section, some concepts about the operational principles and theoretical background regarding fluorescence and optical imaging will be discussed briefly.

Luminescence is "a process in which a luminophore absorbs light to raise an electron from a ground-state level to a excited-state one, followed by a spontaneous relaxation in which the electron returns back to the ground state. In this later transition, a photon with the energy equivalent to the difference between both excited and ground states is emitted" [37]. Within this context, the process is called fluorescence when it is fast and phosphorescence in the case of longer time scales. Fluorescence-based oxygen sensors rely quenching of such luminescence due to interactions with oxygen molecules. The relation between named fluorescence and O_2 concentration is explained by the *Stern-Volmer equation*:

$$\frac{I_0}{I} = \frac{\tau_0}{\tau} = 1 + \tau_0 k_q [O_2] \tag{2.1}$$

where τ_0 and I_0 are the decay time and intensity time in the absence of oxygen, τ and I are the decay time and intensity time at $[O_2]$, and k_q is the Stern-Volmer quenching constant [39]. The result of plotting $\frac{I_0}{I}$ vs $[O_2]$ is a linear plot that allows extrapolation. This relation is not applied to the results obtained in the thesis, since it is not possible with the laboratory equipment to measure intensity in total absence of oxygen due to limitations of the gas control system.

3. MATERIALS AND METHODS

In this section the main equipment and materials used will be described and the methods and protocols followed will be explained in detail.

3.1. Sensor design and fabrication

3.1.1. Reagents

The chemicals used for the phosphorescent membrane are platinum octaethylporphyrin complex (PtOEP, Porphyrin Products Inc., Logan, UT, USA), 1,4-Diazabicyclo[2.2.2]octane (DABCO, 98%), tetrahydrofuoran (THF) and polystyrene (PS, average M.W 280,000). All three were supplied by Sigma-Aldrich Química S.A. (Madrid, Spain).

Polydimethylsiloxane is prepared using the SYLGARD ®184 silicone elastomer kit, provided by SIGMA, with a ratio of 10:1 base to curing agent. Collagen type I solution from bovine skin (C4243-20mL) is bought from SIGMA.

3.1.2. Membrane Assembly

The cocktail for the sensing membrane was prepared by dissolving 0.5mg of PtOEP and 12mg of DABCO in 1mL of a solution of 5% (w/v) PS in freshly distilled THF, according to the protocol described by López-Ruiz et al. [24]. The vials with the cocktail are stored at 4^{o}C in a dark environment until use.

Two different containers are used to assemble the sensing membrane (Fig. 3.1), a circular glass plate of 30mm diameter or an 8-well plate (Thermofisher, well size 1x0.8cm). Figure 3.2 shows the different layers that are deposited.

Firstly, the cocktail containing the luminophore is casted on the glass plate and left to dry in a THF atmosphere for 24h. For the round dishes (ϕ 30mm), 0.5mL are deposited, resulting in a thickness of $13 \pm 0.29 \mu m$. For the 8-well plates, 0.3mL are deposited on each well. The resulting membranes are transparent and pink in color. However, the surface is not homogeneous, presenting a thicker layer around the edges and scattered spots. As

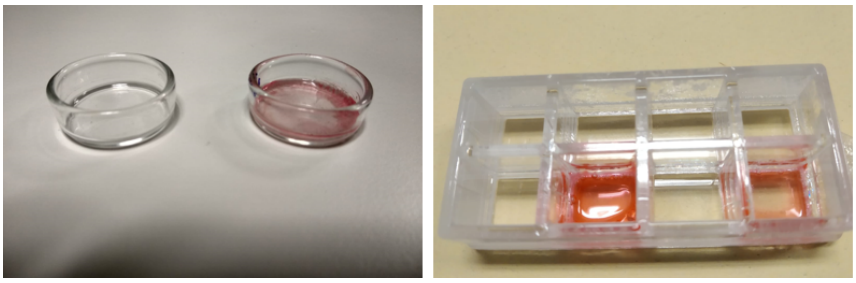

Fig. 3.1. Different membrane fabrication sizes. Left: round plates. Right: rectangular wells

a result of this, the fluorescence intensity is not the same in all positions of a membrane. The square wells of the 8-well plate provide a more homogeneous layer of PtOEP than the round plates. To address this inhomogeneities, average pixel intensity of each image is calculated.

For PDMS preparation, mixture is prepared with a ratio of 10 parts base to 1 part curing agent. It is subsequently placed inside a vaccuum chamber to remove air bubbles introduced. Then a layer is poured on top of the porphyrin membrane (0.9g in the round plate, 0.2g for the rectangular wells) and cured for 48h in a dark environment with circulating air.

Finally, the surface is sterilized and subsequently functionalized to promote cell adhesion. A volume (2mL round plate, 0,2mL rectangular well) of a 1:20 solution of collagen type I from bovine skin in PBS is poured in the plate and left for 2 hours under UV light. After this time, the excess liquid is aspirated and the sensor is ready for use.

Fig. 3.2. Sensor assembled layers in a petri dish

3.1.3. Microscopy equipment

All images are accquired using Leica DMi8 Inverted Microscope (Leica Microsystems CMS GmbH, Wetzlar, Germany) and its proprietary software LASX Navigator (Leica

Microsystems). The microscope is integrated with a bioreactor which maintains stable conditions of $5\%CO_2$ and 37ºC suitable for cell survival during the prolonged timelapse experiments. The setup is shown in Fig. 3.3.

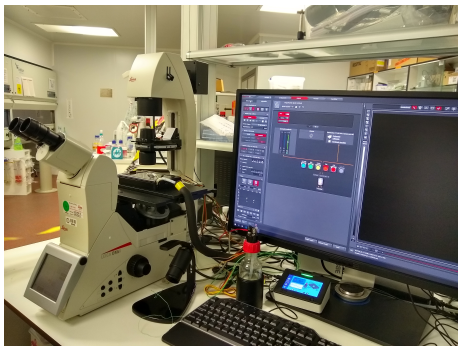

Fig. 3.3. Microscope setup

Figure 3.4 shows the software with the different settings that can be adjusted. The large square on the right corresponds to the visor of the microscope. In the middle section, filters and emission intensity of the lamp can be adjusted. The right section includes all the controls to customize position and acquisition cycles of the timelapse experiments. It also allows to set different values for the z-axis, to focus at different leves, such as the membrane or the cells, depending on the experiment. To image the cells we select the GFP filter. To image the membrane we select the TXR filter, with an excitation spectrum of 545-580nm and an emmission filter of 605-656nm, wavelengths that are close to the maiximum emmision and excitation peaks of the PtOEP complex shown in previously in Fig. 2.6. All membrane images are acquired with an augmentation of 4x.

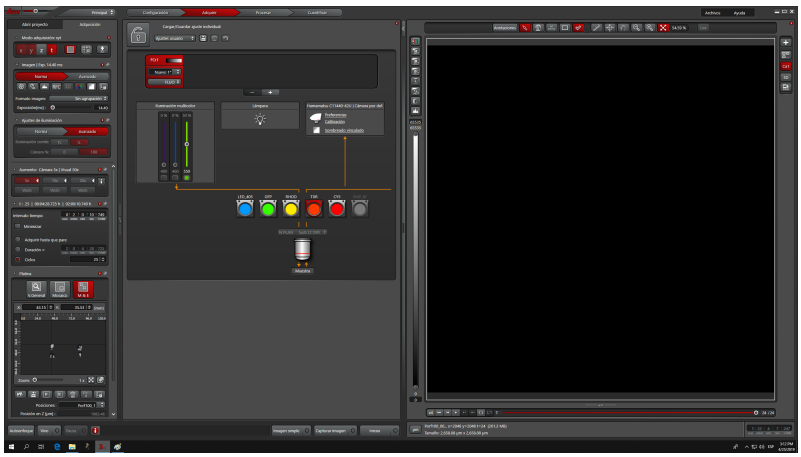

Fig. 3.4. LAS X software

3.2. Cell culture protocols

Green fluorescent HaCaT cells (HaCAT-GFP), an immortalized human keratinocyte cell line, were used along the whole project. Culture medium is prepared with Dulbecco's Modified Eagle Medium with high glucose content and without sodium pyruvate (DMEM, Invitrogen Gibco) complemented with 10% FBS (Fetal Bovine Serum, Thermo Scientific HyClone) and 2% antibiotic/antimycotic solution (Thermo Scientific HyClone). Cells were grown in an incubator at 37ºC, with an atmosphere of 5% CO_2 and 95% air at a relative humidity of 38%.

Once the cells reached 90% confluence, they were divided in subcultures according to the following general protocol:

1. Culture medium is removed and cells are washed with PBS.
2. 1mL of trypsin is added in each p100 plate. Then, they are incubated for 10 minutes at 37ºC.
3. 5mL of medium are added to inactivate trypsin, cells are resuspended carefully using a pipette. The resulting liquid is introduced in a 15mL Falcon tube.
4. The tube is centrifuged at 1000rpm for 7 minutes.
5. Supernatant is removed and fresh medium is added. Pellet is resuspended.
6. Cells are counted and seeded in culture plates at 1/8 density.

For all experiments in which a certain seeding density is required, cells are counted according to the following protocol:

1. Using a micropippete, $10\mu L$ of the cell suspension are placed in a hematocytometer (Neubauer chamber).
2. Under the microscope, cells in each of the four quadrants are counted.
3. Number of cells per mL of suspension is calculated according to the following formula: # cells per mL = cells $\cdot \frac{1}{4} \cdot 10^4$

3.3. Experimental development

The general setup of the experiments, as described along the previous section, is shown in Fig 3.5. The different layers are added or removed according to the needs of each experiment. The methods followed for each experiment are described in detail in this section.

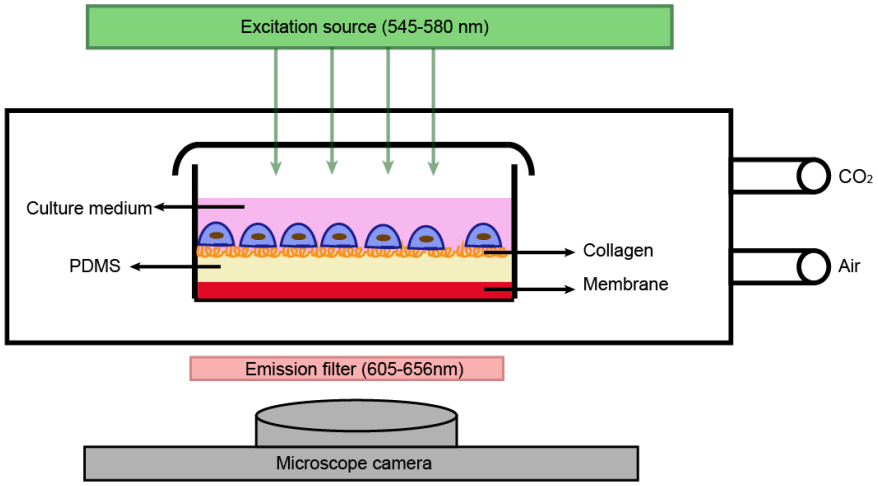

Fig. 3.5. Experimental setup

3.3.1. Cell adhesion

One of the necessary processes for keratinocyte survival is that they adhere to the culture substrate. To obtain an adequate surface for cell culture, the porphyrin membrane was covered with PDMS. Since this material is intrinsically hydrophobic it results in poor cell adhesion and proliferation. To counteract this problem, the surface was functionalized with collagen. To evaluate efficiency of this method, six sensors were prepared (2x membrane+PDMS+collagen, 2x PDMS+collagen, 2x traditional culture dish), shown in Fig. 3.6. All of them were seeded at confluence and incubated for 24h After this time, medium was extracted with a pipette and collected in a different plate. The number of cells present in the media, which had therefore not attached to the substrate, was counted using a hemocytometer. Adhered cells were also inspected microscopically.

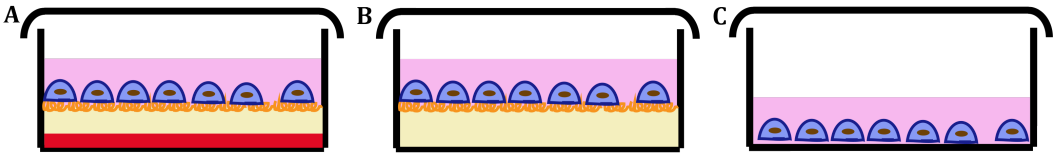

Fig. 3.6. Three different configurations used in cell adhesion experiment. A: membrane + PDMS + Collagen. B: PDMS + Collagen. C: traditional petri dish

3.3.2. Cytotoxicity Assay

alarmarBlue® is a commercial assay that allows to measure quantitatively the proliferation of cells. It is based on a fluorometric/colorimetric indicator of metabolic activity. It incorporates an oxidation-reduction indicator that fluoresces and changes color in response to the reduction of growth medium resulting from cell growth. It is demonstrated to be minimally toxic to cells and outputs a clear, stable and distinct signal [43].

In order to perform this cytotoxicity assay, cells are seeded at 80% confluence in round plates (30 mm diameter) with the three following relevant configurations:

- G1 (Membrane + Microscope): Three plates mimicking experimental conditions, including the sensing membrane and placed under the microscope for four days, with periodical fluorescence excitation cycles.

- G2 (Membrane + Incubator): Three plates with the sensing membrane placed inside the incubator, in a dark environment, for the duration of the experiment.

- G3 (No membrane + Incubator): Three glass plates without sensing membrane placed inside the incubator for the duration of the experiment.

Reaction medium is prepared with 10% alarmarBlue® and 90% DMEM without phenol red. The resulting solution is mixed and filtered. All these procedures are carried out in darkness conditions.

To perform the experiment, culture media is aspirated and cells are washed with PBS. Subsequently, 2mL of reaction media are added to each plate and incubated for 3 hours, every group in the same conditions (darkness). Then the alarmarBlue® solution is removed from the plates and placed in a 96-well plate for analysis, using EMax® Plus Microplate Reader from bioNova cientifica. Data of absorbance at 570nm and 600nm

is given, corresponding to the reduced and oxidixed excitation wavelengths respectively. This prodedure is carried out at three different time-points:

Day 0 (24h after cell seeding) - Day 1 - Day 4

Data processing is carried out using the absorbance data in the following formula:

$$\%Reduced = \frac{(\epsilon_{ox})\lambda_2 \cdot A_{\lambda 1} - (\epsilon_{ox})\lambda_1 \cdot A_{\lambda 2}}{(\epsilon_{red})\lambda_1 \cdot A'_{\lambda 2} - (\epsilon_{red})\lambda_2 \cdot A'_{\lambda 1}} \tag{3.1}$$

Where $(\epsilon_{ox})\lambda_1$ is the oxidation extinction coefficient for 570nm (80,586); $(\epsilon_{ox})\lambda_2$ is the oxidation extinction coeffiecient for 600nm (117,216); $(\epsilon_{red})\lambda_1$ is the reduction extinction coefficient for 570nm (155,677); $(\epsilon_{red})\lambda_2$ is the oxidation extinction coeffiecient for 600nm (14,652) $A_{\lambda 1}$ and $A_{\lambda 2}$ are the readings at 570 and 600nm respectively; $A'_{\lambda 1}$ and $A'_{\lambda 2}$ are the readings in the controls without cells at 570 and 600nm respectively.

3.3.3. Photobleaching

Photobleaching is a process by which the repeated cycling of a fluorophore between ground and excited states eventually leads to molecular damage with a gradual reduction of fluorescence emission intensity from a sample over time [44]. This phenomenon is specifically of interest for time-lapse microscopy experiments, such as the ones presented in this project, as alterations of the fluorophore might lead to inconsistent data over time. For this experiment, samples are placed under the microscope with excitation cycles every two hours during 64 hours, mimicking experimental conditions. Pixel intensity is analyzed in images.

3.3.4. Oxygen level studies

The general idea of these experiments is that oxygen concentration is changed in the chamber of the bioreactor and the response of the sensor is analyzed. The main challenge is linked to the limitations of the gas control system, which does not provide stable concentrations over time and only allows to change O_2 concentration within a narrow range, as it is intended for regular cell culture. For all experiments, oxygen levels were changed within the constrictions of the microscope equipment, resulting in five different oxygen concentration values (18,27%; 18,9%; 19,95%; 20,58% and 21%).

Experiment 1: two sensors in round plates were used, taking images from three different positions in each of them. In this scenario, only the porphyrin layer was deposited on the glass plate, being the fluorophore directly exposed to the environment. Measurements started at 21% O_2, progressing downwards and waiting for five minutes in between changes to account for chamber stabilization time. Three consecutive images were taken for each position at each O_2 level to obtain a value for the variability.

Experiment 2: PDMS is known to be highly permeable to oxygen. Despite this fact, it was a concern whether the layer of PDMS would allow enough (or fast enough) pass of the gas for the sensor to be able to detect changes. With the aim of exploring this, 3 glass round plates were prepared with the porphyrin membrane. The same procedure as in the previous experiment was followed. After image acquisition, the PDMS layer was deposited and, after 48 hours of curing, images were acquired again. Same positions could not be maintained in between experiments and therefore the DC levels are not comparable between the two days.

Experiment 3: cells in culture are not directly in contact with air, they are covered with the nutrient-rich culture medium. This fluid allows gas diffusion. In this third experiment, the previous porphyrin+PDMS structure is covered with cell culture medium to compare the measurements obtained. The same changes in gas concentration are applied.

Experiment 4: membranes were placed under the microscope according to the configuration shown in Fig. 3.7. Samples were monitored every 30 seconds. In this way, images can be acquired quasi-simultaneously above and below the cell culture medium layer, potentially allowing to study oxygen diffusion across this fluid.

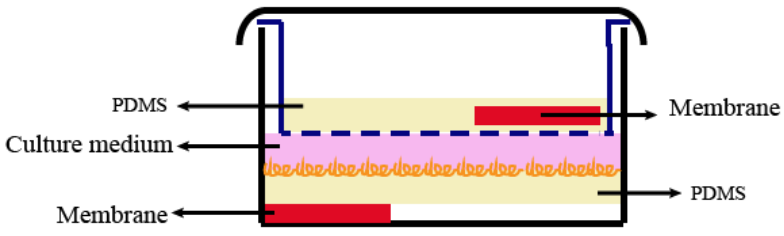

Fig. 3.7. O_2 diffusion across culture medium: Transwell set-up

Experiment 5: For this experiment, 1 hour (instead of five minutes) was waited in between O_2 concentration changes. Images were acquired every 15 minutes, to monitor

the evolution of fluorescence intensity. Three different conditions were monitored (naked membrane, membrane+PDMS and membrane+medium) in both plates, with and without lid.

3.3.5. Cell density studies

Two different experiments were carried out using each type of membrane shape (round plates and square wells). In both cases, four sensors were prepared, three of them seeded with cells (100%, 80% and 40%) and a control without cells. Three repetitions of each image were acquired. For cellular experimentation, cells are seeded 24 hours prior to the begining of the experiment. Culture medium is removed just before the beginning of image acquisition and repleaced with fresh medium without phenol red.

3.3.6. Cell migration study

A scratch assay is performed. To do so, cells are seeded in round plates at 100% percent confluence. After 24h of incubation, a scratch is performed by "scraping" the cell monolayer using a pipette microtip to make a straight line. The cell front is imaged along 14 hours, acquiring pictures of both the cells with the GFP filter and the sensor (n=4). Images are taken every 2 hours.

3.4. Image analysis

Once image acquisition process is finalized, pixels in these images need to be analyzed to quantitatively determine fluorescence intensity. This processing is carried out in MATLAB.

First, the images are loaded and the average of all the pixels in each image is calculated, providing a single intensity value for each image. Other strategies, such as calculating the mode or eliminating the very bright/dark outliers were tried. However, the calculation that best represented the information was the simple calculation of the mean pixel intensity.

3.4.1. Mask for migration assay

To analyze the migration assay, the code is modified so that a certain threshold is applied at the GFP image, which allows to differentiate between regions with and without cells. Then, this same mask is applied at the analysis of the membrane image, averaging separately pixel intensity of zones with and without cells. An example is shown in Fig. 3.8, which shows the membrane (left), the GFP image of the cells (center) and the mask used to separate the two areas (right).

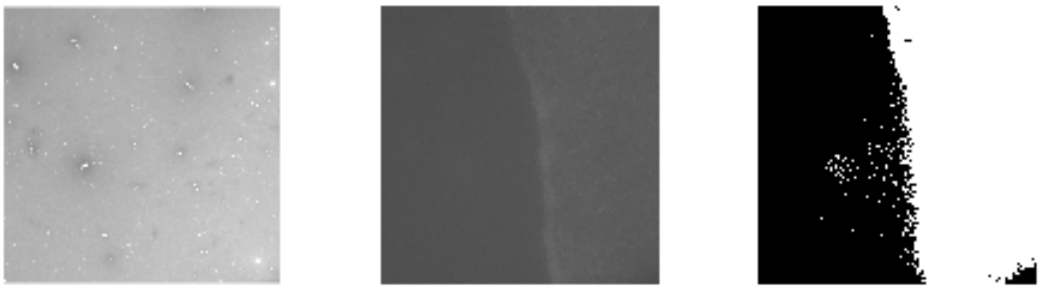

Fig. 3.8. MATLAB Mask for Migration Studies. Membrane image (left), GFP image of cells (center) and mask for separation of areas (right)

4. RESULTS AND DISCUSSION

This chapter will display, analyze and discuss the results obtained in this project. The first section corresponds to the experiments that allow to characterize the sensor behavior and compatibility with the desired application for cell culture. The second section deals with experiments in which oxygen concentration is changed using the gas control system to monitor the sensor response under different conditions. The two final sections are oriented to measure some parameters related with oxygen consumption and diffusion in cell culture.

4.1. Sensor characterization

In order to ensure that measurements are adequate and accurate, a preliminary phase of sensor testing needs to be carried out to determine cell survival and proliferation under experimental conditions, as well as sensor behaviour along the experimental duration.

4.1.1. Porphyrin membrane baseline fluorescence

The basis of this sensor is a porphyrin membrane whose fluorescence under a certain wavelength is quenched by the presence of oxygen. From preliminary studies, it was noticed that average pixel intensity of images of different samples (or different positions) of the porphyrin membrane displayed a large variation at the same oxygen concentration. Therefore, although intensity variation along time of a specific position does indicate a change in oxygen concentration, absolute values of intensity cannot, in principle, be compared between different areas or sensors.

To address this issue, the experiments were set up in such a way that variations within the same position could be calculated. Furthermore, transversal to the whole project, a solution that provided more homogeneous intensity levels among different sensors was searched. The initial sensors fabricated in round glass plates (diameter=30mm) were substituted by square wells, which resulted in a thicker porphyrin membrane with a lower volume of cocktail used. Fig. 4.1 displays the different structures observed with the

microscope (5x augmentation). It is observed that the thicker and smaller membranes of the rectangular wells are more homogeneous, presenting less spots than for the case of the original round plates. Six images from each of these two different configurations are acquired, and the variability among them is studied (Table 4.1). The standard deviation is greatly decreased with the change from the round plates to the square wells (from 15% to 0,8%).

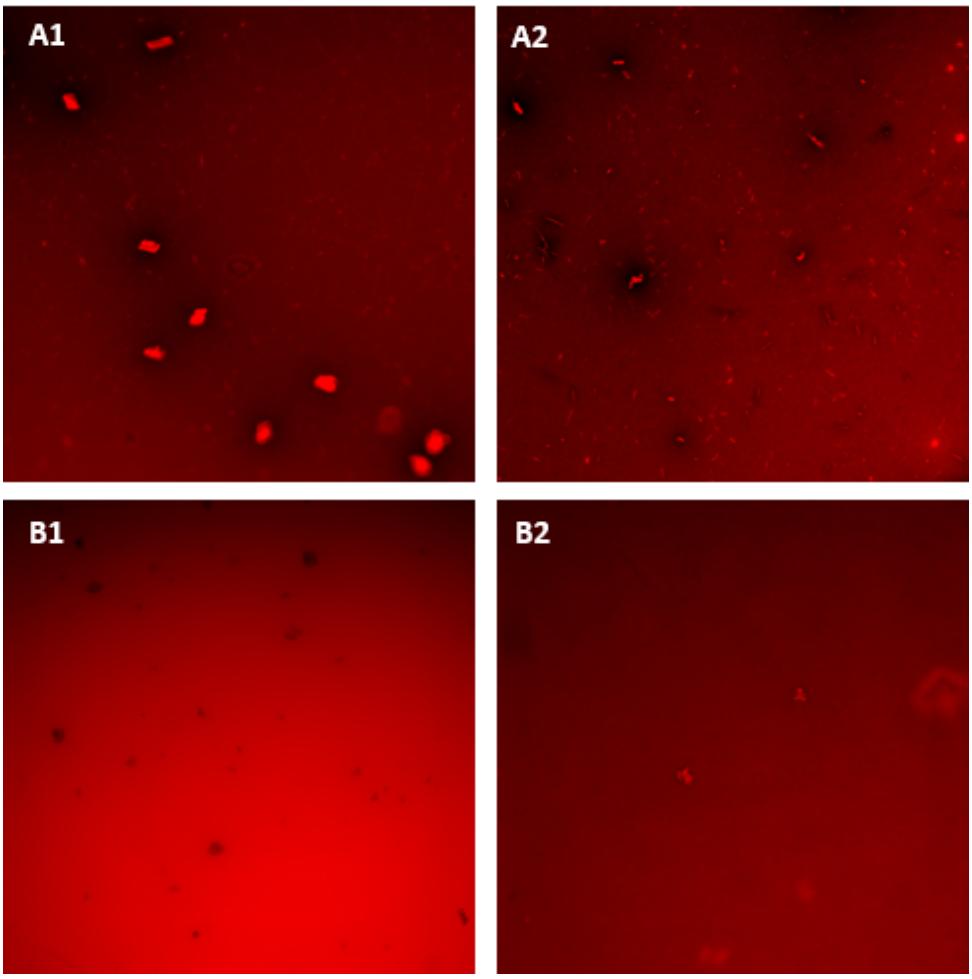

Fig. 4.1. Different membrane fabrication sizes: membrane images. Round plates (A1, A2), rectangular wells (B1, B2)

Table 4.1. AVERAGE PIXEL INTENSITY VARIABILITY

	Average intensity	Standard deviation	Percent error
Round plates	39903	6113	15%
Rectangular wells	17163	141	0,8%

4.1.2. Cell Adhesion

Cells suspended in the medium were counted (Table 4.2). This number of cells was very low, and comparable to that of regular cell culture plates without coating. This shows that surface functionalization was effective in promoting cell adhesion 24 hours post-seeding. Therefore, for subsequent experiments, cells were left in the incubator for 24 hours before starting any assay.

Table 4.2. ADHESION CELL COUNT

	# of seeded cells per plate (millions)	# of floating cells per plate	% adhered cells
Membrane	2	29167	99 ± 1
PDMS	2	62500	97 ± 1
Control	1,6	43750	97 ± 2

4.1.3. Cytotoxicity

alamarBlue® tests were carried out following the procedure indicated in section 3.3.2. Percent reduction was calculated for the three different groups and is shown in figure 4.2. A growing trend is observed from day 0 to day 1, which indicates cell proliferation in all experimental groups. For G1 and G3 a slight decrease in reduction occurs at day 4, which is explained by the fact that, four days after seeding, the cells had already reached confluence and cellular activity decreased.

Overall, the results of this experiment indicate that neither the porphyrin membrane nor the illumination in the microscope kill or harm the cells.

4.1.4. Photobleaching

Figure 4.3 shows the evolution of the mean pixel intensity of images taken every two hours for 64 hours in three different samples (3 positions per sample).

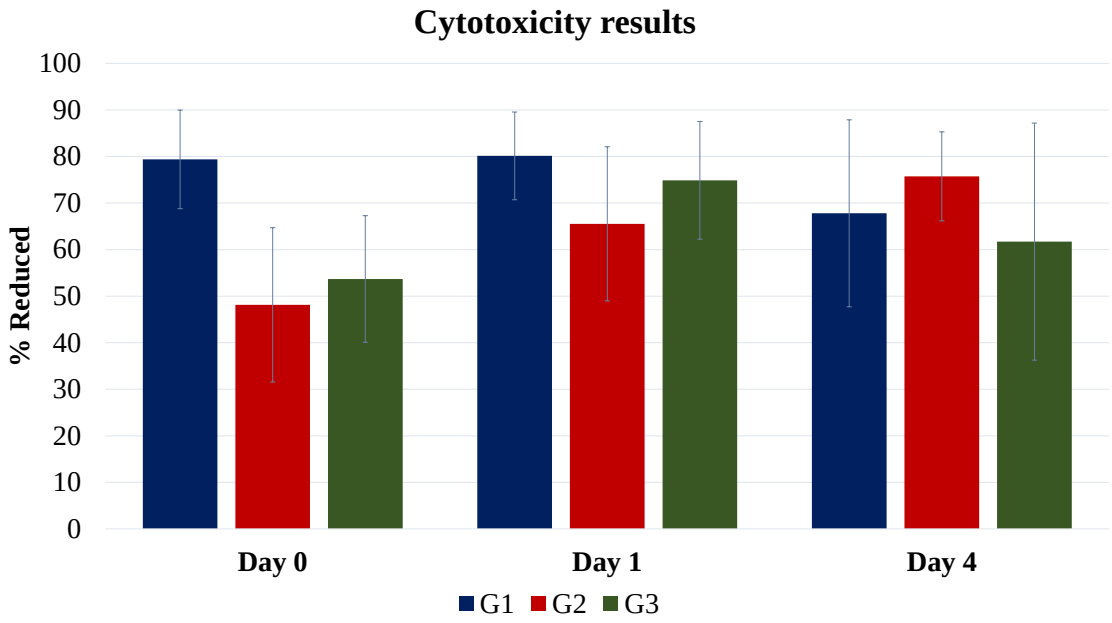

Fig. 4.2. alamarBlue® results: Percent reduction. G1: plates with membrane and under microscope illumination. G2: plates with membrane kept in the incubator. G3: plates without membrane kept in the incubator

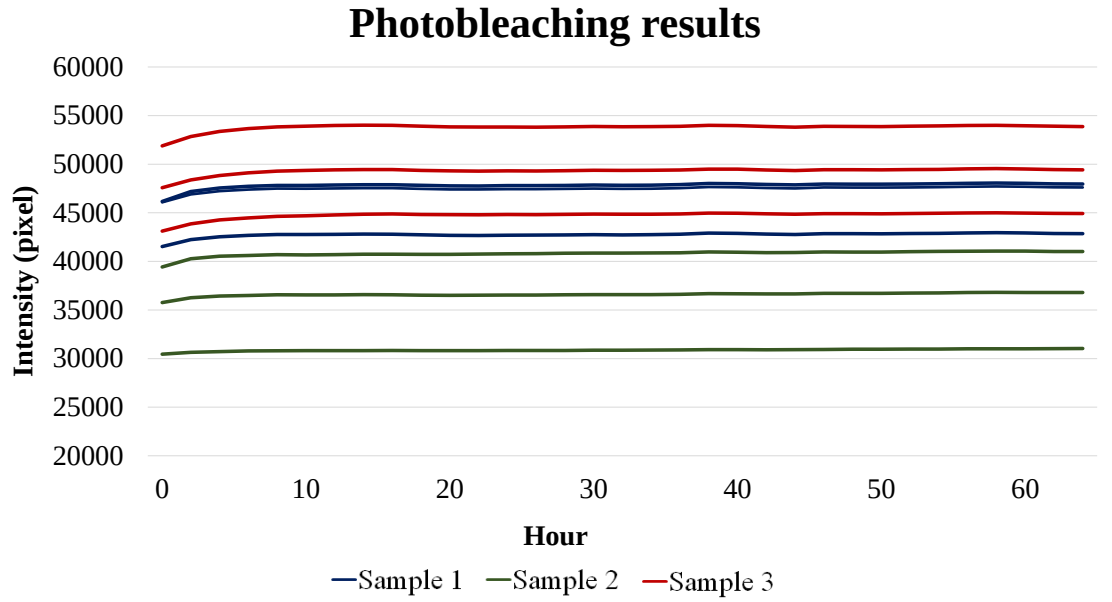

Fig. 4.3. Evolution of pixel intensity over 64 hours on three samples, three positions per sample

The following aspects are observed:

- The response is very flat along the whole experimental duration. The response of the sensor is stable over 64 hours, with excitation cycles every two hours.

- The largest variation within each sample is observed from t=0 to t=2h. This is explained as the stabilization time necessary for the sensor in the bioreactor of the microscope.

- Variability is observed among the DC level of the response of each position, even within the same sample, due to the heterogeneity of the surface resulting from the fabrication proccess.

Several important conclusions are drawn from the aforementioned observations that affect the set up of further experiments in this study:

- Photobleaching does not occur with the present experimental conditions. This will be the maximum experimental duration explored in this project and further tests should be done in this regard if longer time-lapses were to be done.

- The larger variation among the first few images of the experiment is repeated over all time-lapse procedures in this project and, therefore, the first images acquired in each experiment are not taken into account for further analyses.

- As presented in subsection 4.1.1, the response of the membranes is not homogeneous, so as a result intensity levels of two different positions cannot be directly compared to each other. This result will be important for further experiments in this project, as it greatly restricts the experimental setups that can be considered.

4.2. Oxygen level studies

Once the cytocompatiblity and stability of the sensor is established, the sensitivity of the sensor to oxygen level variations was studied with several different approaches.

Experiment 1: proof-of-concept

Figure 4.4 shows the results of the average intensity values for different oxygen pressures. Error bars, calculated as the standard deviation of the images taken for each position, are not visible in the graph as they are of the order of ± 10 while intensity values are of the order of $\pm 10,000$. Figure 4.5 combines the average intensity of all the zones for each oxygen level.

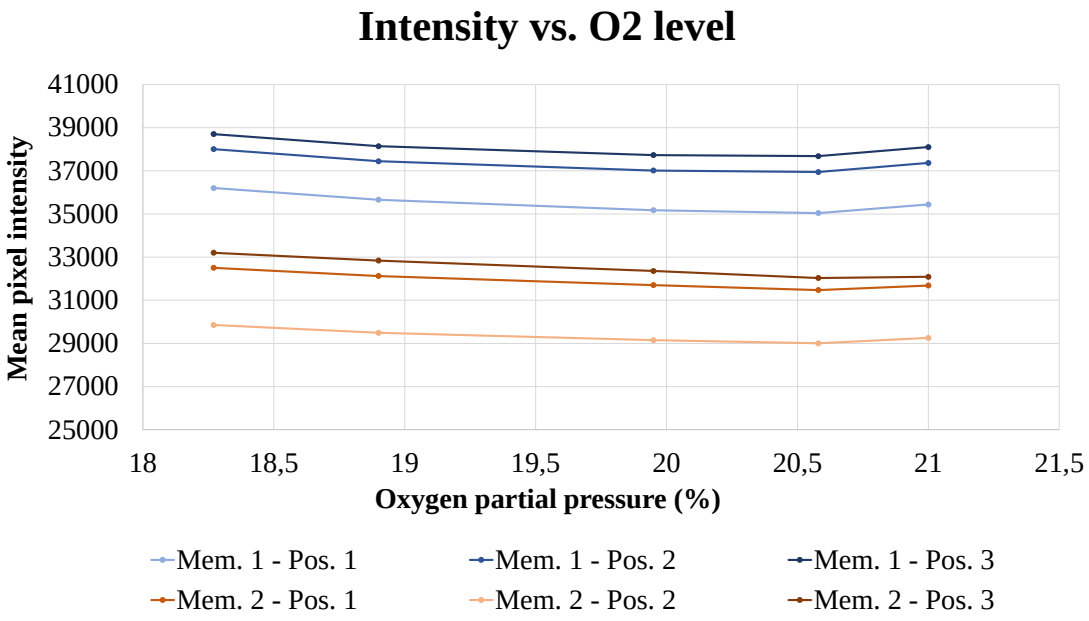

Fig. 4.4. Evolution of pixel intensity versus oxygen partial pressure in two membranes, two poistions per membrane

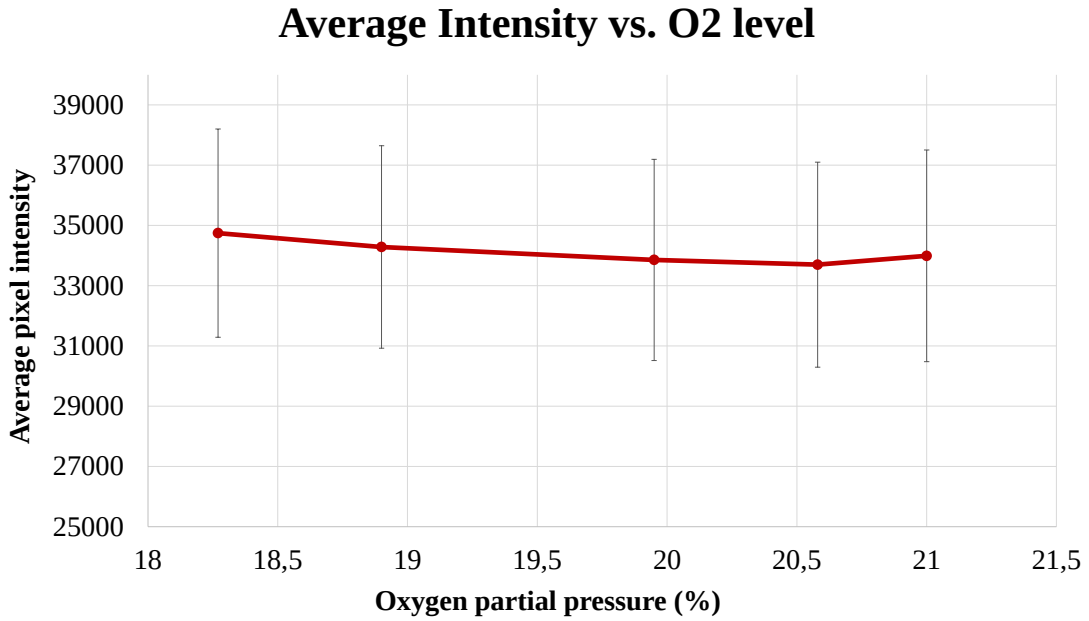

Fig. 4.5. Pixel intensity versus oxygen partial pressure. Average of all positions from Fig. 4.4

Despite the large error bars consequence of the variations in DC level intensity between the different positions, it can be clearly observed that intensity decreases as oxygen partial pressure increases. Intensity at 21% oxygen is slightly higher than at 20,58%. This can be explained by the fact that it was the first image taken and, as was detailed before the

first measurements are usually not accurate enough.

This is a very positive result, as it shows that the fabrication protocol leads indeed to a sensor that is able to detect small differences in environmental oxygen concentration.

Experiment 2: effect of PDMS

Figure 4.6 shows the results obtained for both configurations. Same positions could not be maintained before and after the PDMS layer, so absolute values of intensity levels are not comparable between the two lines. Both sensor configurations follow the same trend, with lines with a very similar slope. The behavior of the sensor with the added PDMS layer is comparable to the one without it, which leads to the conclusion that this material allows free passage of oxygen and will not affect further measurements.

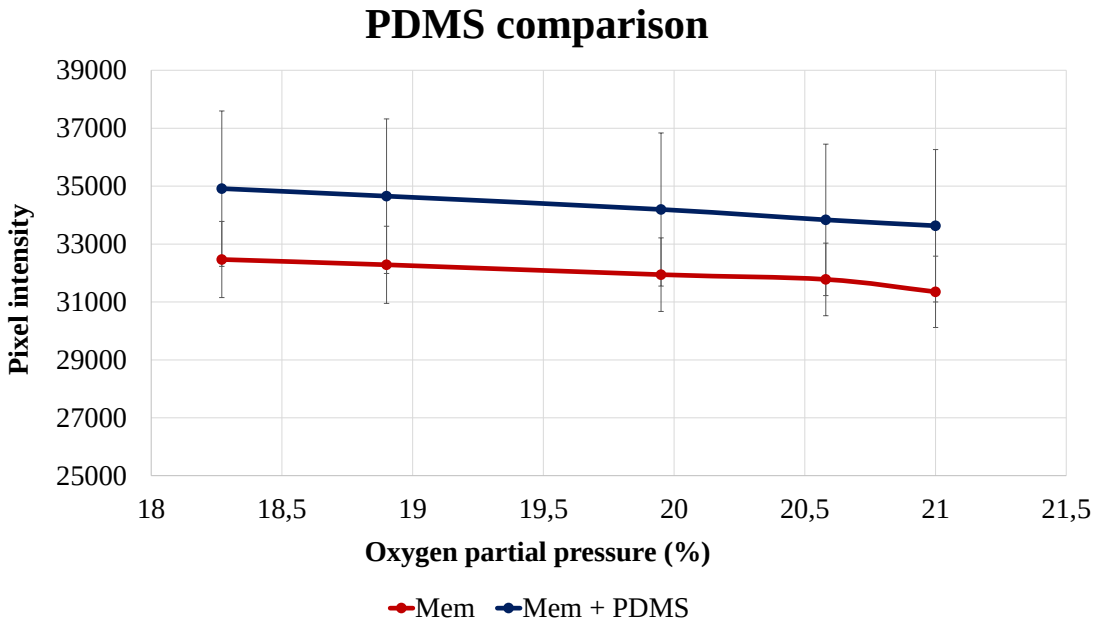

Fig. 4.6. PDMS study: Average pixel intensity versus oxygen partial pressure comparison

Experiment 3: effect of cell culture media

The membrane layers are covered with culture medium, obtaining the results shown in fig. 4.7. The response of the sensor which is covered with culture medium is almost flat, clearly different from the trend observed in previous experiments. This is explained by the fact that diffusion across it is much slower and five minutes is not enough. Culture medium, as well as providing nutrients for the cells, provides a somewhat stable environment, protecting them from sudden changes in environmental oxygen concentration.

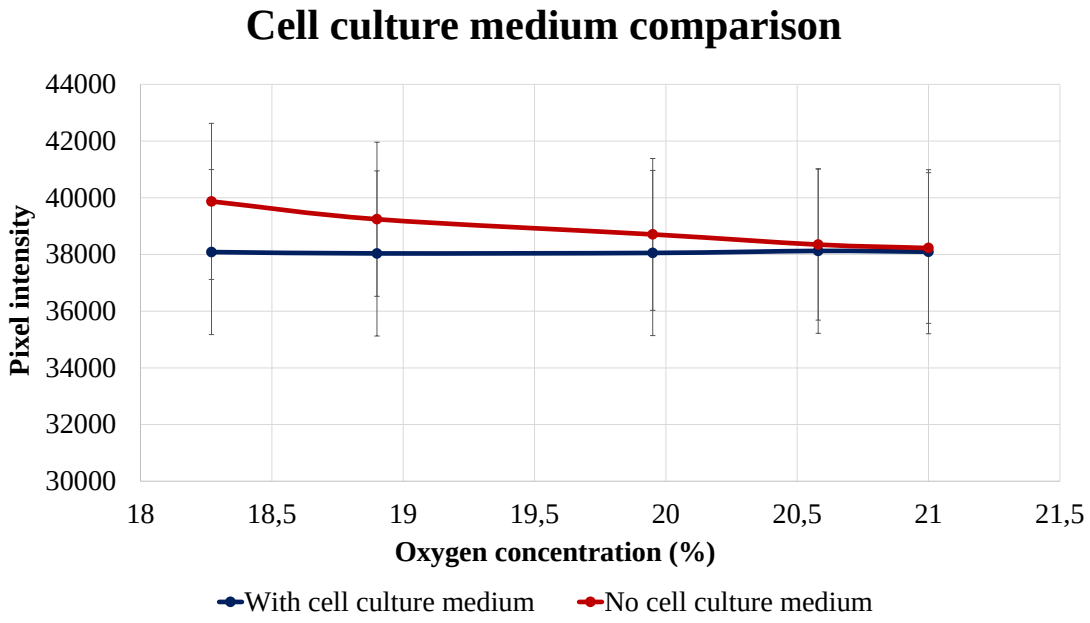

Fig. 4.7. Comparison between sensor with and without cell culture medium

Experiment 4: constant monitoring and diffusion across media

To further explore the sensor behaviour, another experiment was performed in which the samples were monitored during the whole process with images every 30 seconds. The aim of this experiment was to check whether the oxygen level stabilized in the sample and the response time of the sensor, placing membranes above and below cell culture medium as shown previously in Fig. 3.7.

Figure 4.8 shows the evolution of the average pixel intensity of the images over time, as O_2 partial pressure increases. Each different coloured section begins at the time at which O_2 concentration was modified. Regarding the measurements above culture medium, the following conclusions are extracted from this result:

- Emphasizing the results of the previous experiments, a decrease in fluorescence is observed as O_2 partial pressure increases.
- The measurements at the lowest O_2 concentration do not follow the same trend as the rest. Again, these were the first images images taken. Even though the chamber was left to stabilize for a few minutes prior to beginning image acquisition, the unstable results are still observed.
- The response of both the gas chamber and the sensor is fast, as the change in slope

is already present 30 seconds after the change in gas concentration is indicated at the gas control system.

- At the beginning of each 5-minute block the change in pixel intensity is fast, while it progressively slows down and stabilizes towards the end. This shows that the sensor is able to stabilize in this time

Ideally, the sensor below the culture medium would display the same shape as the upper one but later in time. However, it can be seen that the response does not follow a clear trend. This result could be expected by looking at the conclusions from Experiment 3, as five minutes is not a long enough time for diffusion across the liquid.

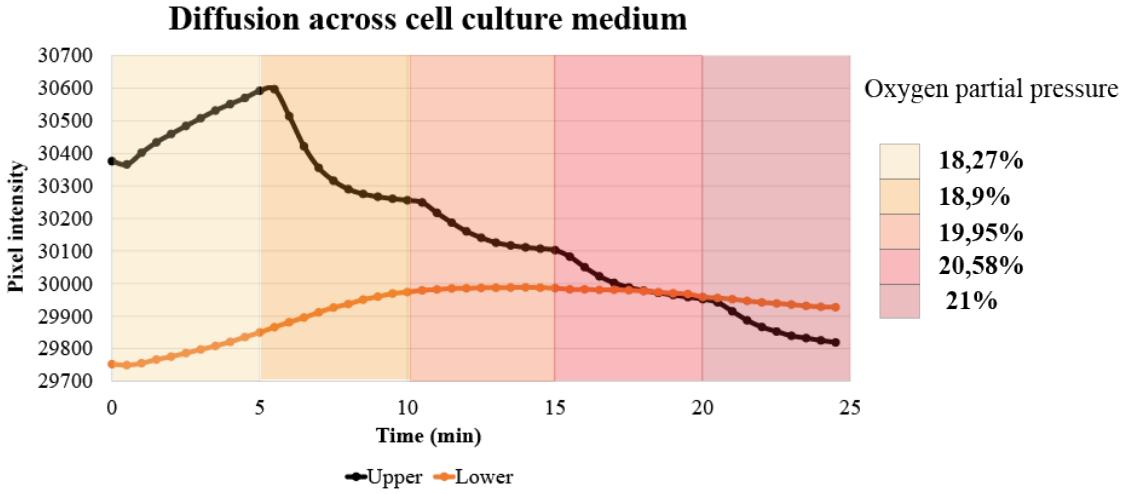

Fig. 4.8. O_2 diffusion across culture medium: Upper and lower sensor compared

Experiment 5: O_2 diffusion across cell culture media

Leading from the previous results, it appeared necessary to perform a test using the sensor covered with cell culture media with a longer experimental time.Results are shown in figure 4.9. The following aspects are observed:

- The lines corresponding to the same condition with and without lid are very similar to each other. This means that the lid doesn't affect the measurements.

- As oxygen concentration increases, fluorescence intensity increases as well. This response is the opposite of what was expected and doesn't correlate with previous results.

The result obtained from this experiment is not considered successful. Since the growing trend is observed in all lines, including those that had already proved to work successfully, the culture medium is not considered to be the problem. Some hypothesis that explain this problem are condensation effects or problems with the gas control system.

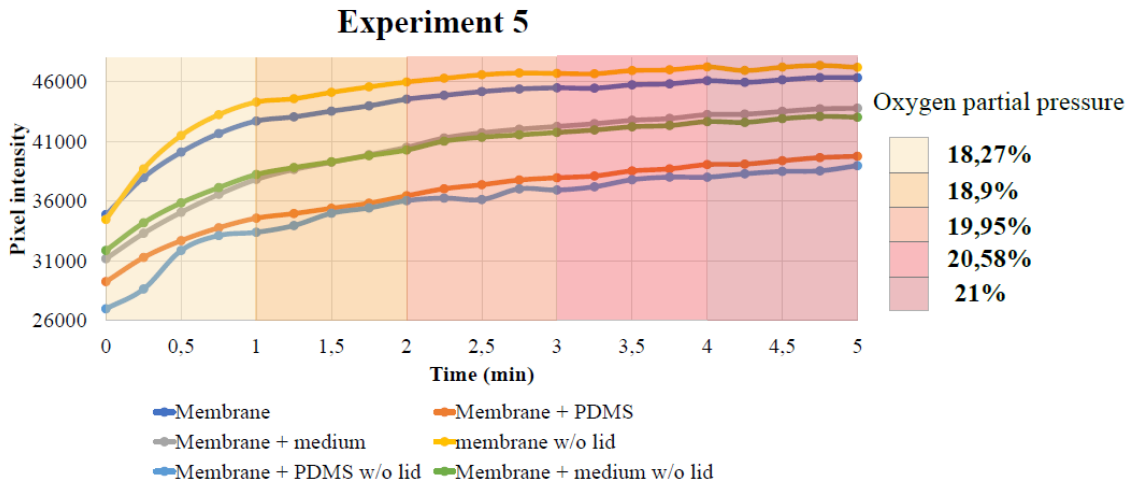

Fig. 4.9. Experiment 5: evolution of pixel intensity vs oxygen partial pressure.

4.3. Cell density studies

During normal metabolism cells consume oxygen, which diffuses from the environment across the culture medium. However, previous research shows that, while at low cell densities diffusion was enough to replace the depleted oxygen, at higher cell densities a significant decrease in the local oxygen concentration was observed [35]. The experiments carried out for this section aim to explore this situation in the context of this sensor, monitoring oxygen concentration for keratinocyte cultures at different densities. Three different cell seeding densities were considered (40%, 80% and 100%) and compared to a control without cells.

Experiment 1: Sensor in round plates

Figure 4.10 shows the evolution of average pixel intensity of each sensor along 44 hours.Error bars cannot be seen in the graph as they are in the order of ±10. The DC level of intensity of each line does not give any information, as it was made clear in previous experiments that this level changes from one position to another. In order to compare these lines, data is process according to the following two steps:

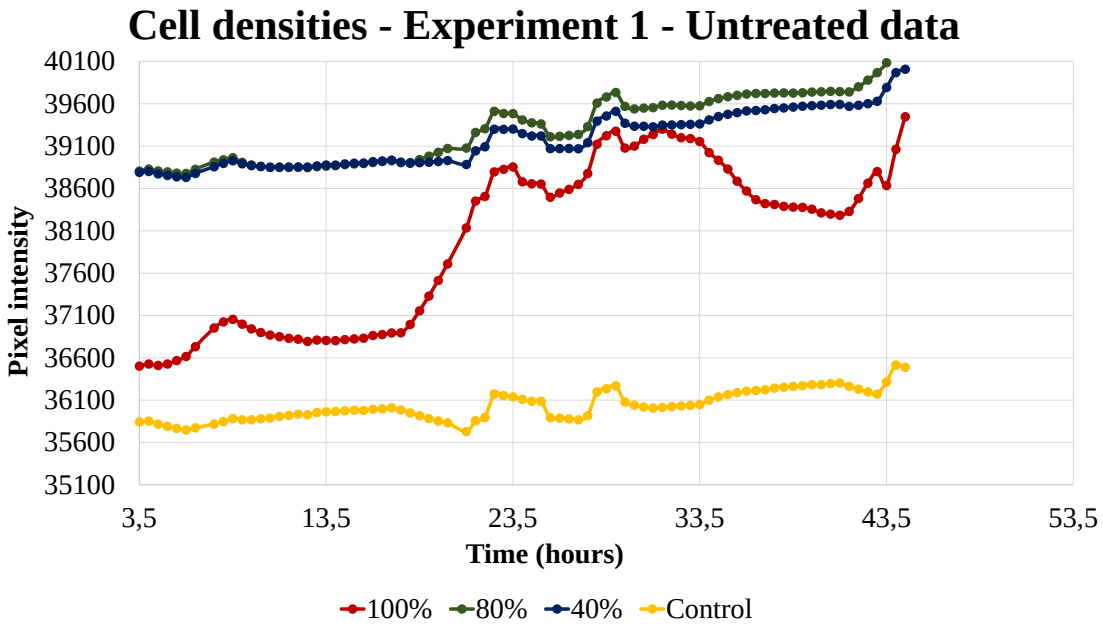

Fig. 4.10. Cell densities Experiment 1 - Untreated data. Graph shows evolution of pixel intensity along 44 hours for: control (yellow), 100% cell density (grey), 80% cell density (orange) and 40% cell density (blue)

1. The difference between each data point and the respective initial intensity of each sensor is calculated ($t_x - t_0$), to visualize intensity variation at each position. Initial intensity is considered as the average pixel intensity at t=3,5h.

2. The value of the control at each time point is subtracted from the value of each cell density: $(t_x - t_0)_{cells} - (t_x - t_0)_{control}$. In this way, oscillations due to the environment are mostly eliminated. They cannot be fully eliminated since each membrane responds differently to gas concentration fluctuations, which are a result of the instability of the gas control system.

Results after this process are shown in figure 4.11. Oscillations in the results are explained by the changes experienced in the chamber of the bioreactor, as the gas control system doesn't allow a very strict accuracy. Despite the drift, it is clear that the greatest increase in pixel intensity is found for 100% cell density. This strongly supports the hypothesis that, at high cell densities, oxygen consumption by the cells cannot be fully replenished with diffusion from the environment.

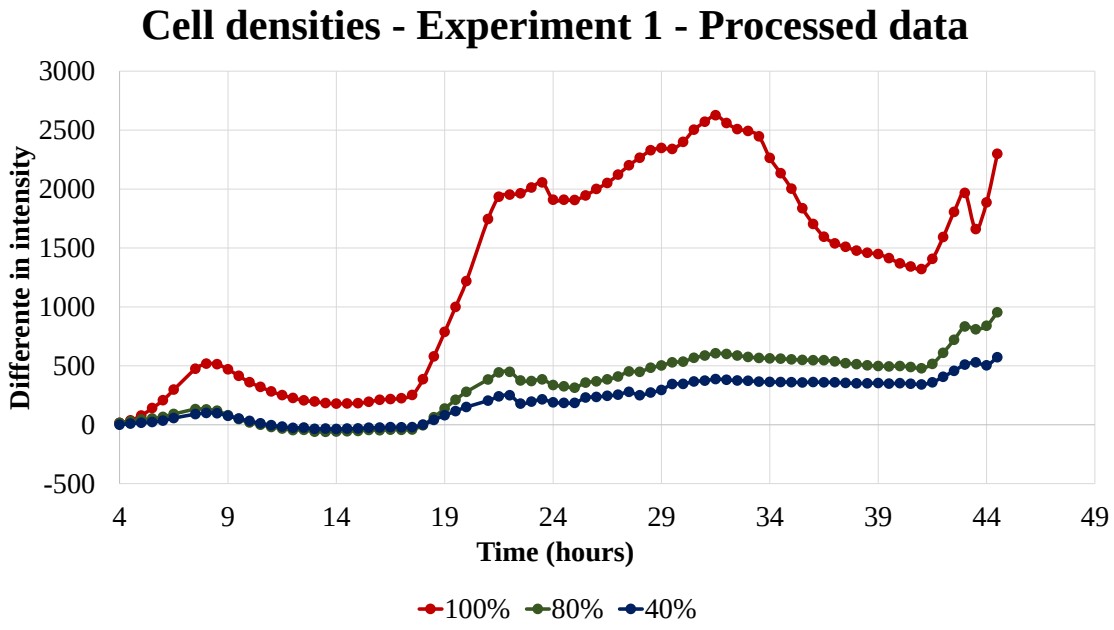

Fig. 4.11. Cell densities Experiment 1 - Processed data. Graph shows evolution of pixel intensity along 44 hours for: 100% cell density (grey), 80% cell density (orange) and 40% cell density (blue)

Experiment 2: Sensor in square wells

For the final round of experiments, square wells were used with the aim of homogenizing the DC level of the results and reducing the amount of oscillations.

The following aspects are noted from the results obtained (Fig. 4.12):

- The first three acquired images are not analyzed. This time is accounted for as stabilization time. Therefore, the graph begins at t=6 hours.

- The DC level of the control is the lowest one, followed by the well at 40% confluence. Wells at 80% and 100% confluence are above them, very close to each other. This order is maintained in all three repetitions of the experiment. The fact that the lines corresponding to 80% and 100% are very similar, is explained because, in such small surfaces, the difference in cell number between this percentages is low. Also, the wells are seeded at these confluences 24h prior to the start of the experiment, and therefore some proliferation is expected by the time image acquisition begins.

- All the lines follow the same growing trend, including the control. This means that the increased intensity is not a result of oxygen consumption by cells. This aspect

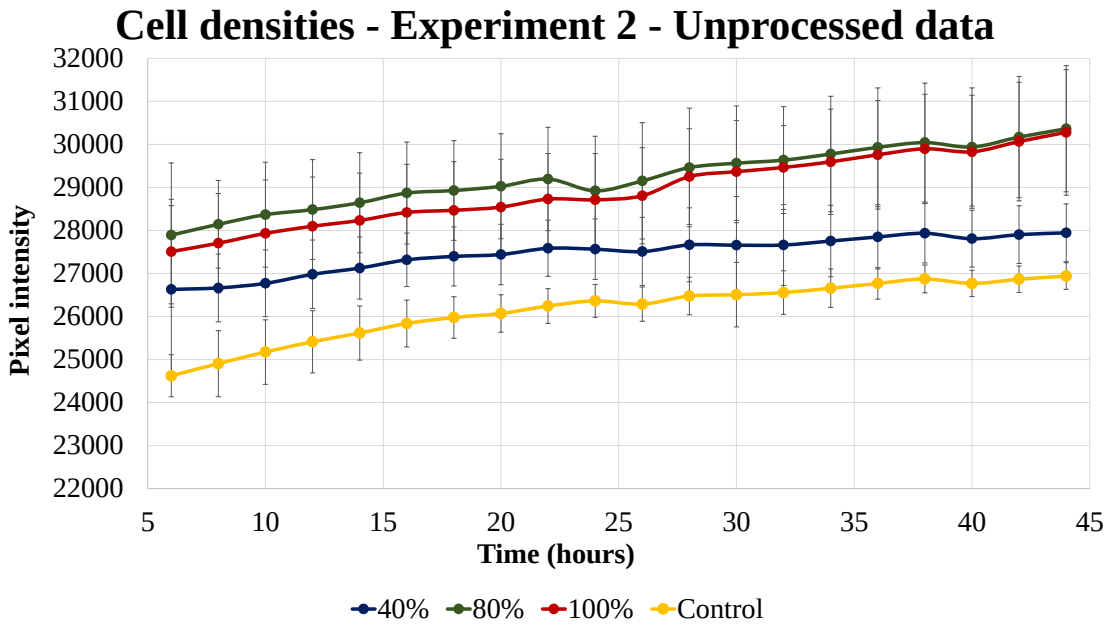

Fig. 4.12. Measurement of pixel intensity at different cell densities. Graph shows evolution of pixel intensity along 46 hours for: control (yellow), 100% cell density (grey), 80% cell density (orange) and 40% cell density (blue)

will be later discussed in more depth.

To follow the same logic as the previous experiment, the same processing algorithm is applied to the data. Obtained results (Fig. 4.13) show that there is a decrease in average pixel intensity over time, meaning an increase in oxygen concentration. It is true that this increase is smaller in the wells with higher cell density and one could argue that, while there is a generalized growth of oxygen concentration, reduction in concentration due to cell metabolism is still observed. However, this trend is observed in the three separate repetitions of the experiment, and therefore it is not likely to be related to changes in gas concentration due to the gas control system of the bioreactor.

These experiments demonstrate that the porphyrin sensor allows to determine variations in dissolved oxygen concentration in a two-dimensional keratinocyte culture. The result supports the idea introduced by previous research that oxygen consumed by cells during metabolism is not fully replenished by diffusion from the environment. Further studies could allow to experimentally determine oxygen diffusion rate across culture medium and point at optimal conditions for cell growth.

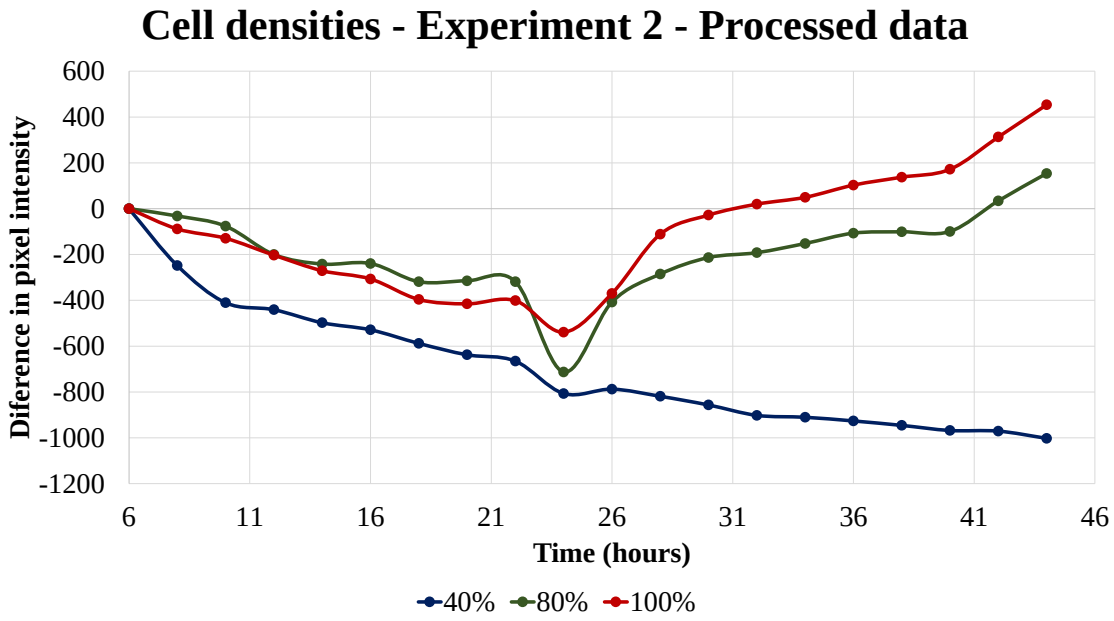

Fig. 4.13. Measurement of pixel intensity at different cell densities. Graph shows evolution of pixel intenisty along 46 hours for: control (yellow), 100% cell density (grey), 80% cell density (orange) and 40% cell density (blue)

4.4. Cell migration study

The porphyrin sensor provides a measurement of local dissolved oxygen concentration. The aim of this experiment is to acquire an image that contains sections with and without cells and monitor oxygen concentration in both areas, to determine whether any difference is percieved. Fig 4.14 shows the evolution of the cell front at 0h, 6h and 14h.

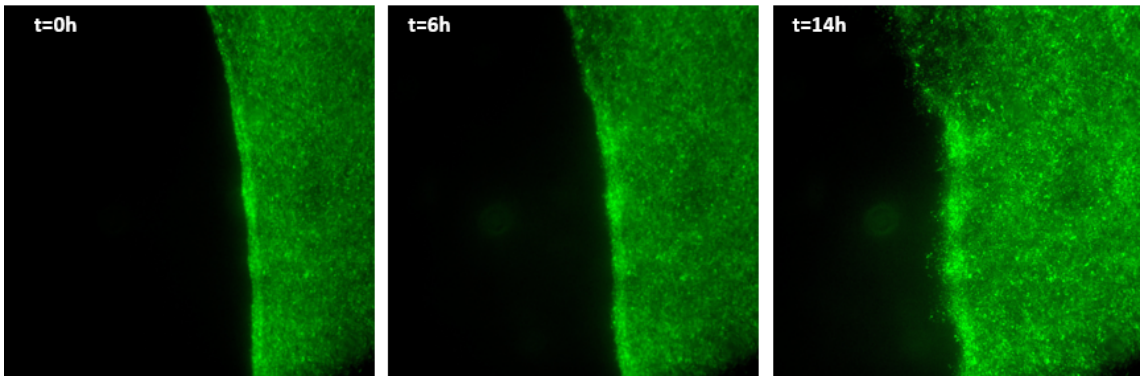

Fig. 4.14. Cell Scratch Assay: Cell Front. From left to right, images of the cell front at 0h, 6h and 14h

To process the images of the porphyrin sensor, data from the parts with and without cells of the imaged are separated. Figure 4.15 shows the results obtained. It is clear that the line corresponding to the area with cells is above the line of the area without cells, meaning that oxygen level is lower in the former. Large error bars are due to variations in the DC levels of intensity among different positions, but the trend is repeated in every of them separately.

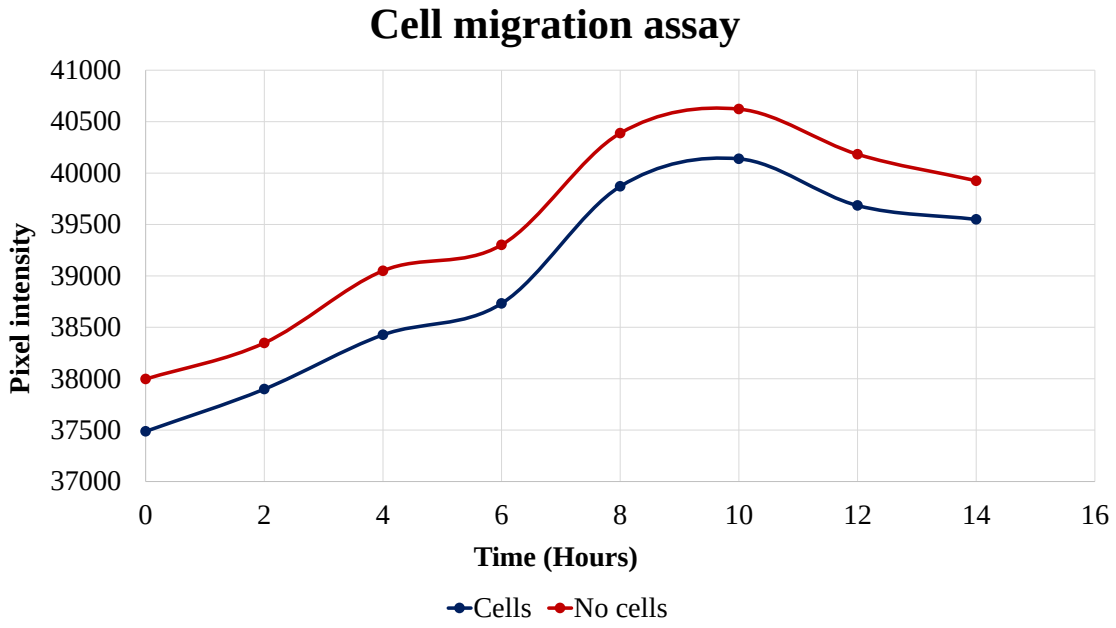

Fig. 4.15. Cell Scratch Assay: Pixel intensity

From these experiments, it is concluded that the porphyrin sensor is able to provide precise measures of local oxygen concentrations, even within the same image.

5. CONCLUSION AND FUTURE PERSPECTIVES

5.1. Conclusion

This thesis has been focused on the development of an optical sensor, specifically its application for determination of dissolved oxygen concentration in two-dimensional tissue cultures. The following conclusions are reached:

- The PtOEP membrane coated with a collagen-functionalized layer of PDMS is fully cytocompatible, as it allows cell adhesion and proliferation.
- The response of the PtOEP membrane under periodical cycles of excitation along an experimental duration of 64 hours is constant, which implies that photobleaching does not occur.
- The PtOEP membrane responds to excitation in the range of 545-580nm with a fluorescence signal which is quenched in the presence of oxygen. Therefore, a PtOEP membrane is an effective method for [O_2] determination.
- A fabrication method that results in smaller and thicker membranes yields more homogeneous intensity levels in different positions within the same membrane.
- At high cell densities, cells consume O_2 from the medium at a higher rate, which cannot be replenished by diffusion from the environment. The PtOEP sensor allows to visualize this increased O_2 consumption of higher cellular densities.
- The PtOEP sensor gives a value of local dissolved O_2 concentration, which allows to differentiate between areas with and without cells.
- An in-depth understanding of the sensor is achieved, which has allowed to set the bases for the design of experiments to measure oxygen diffusion in 3D systems.

Overall, the main goal was attained, as the work on the development and characterization of the sensor has resulted in successful experiments regarding measurements of O_2 concentration in cell culture.

5.2. Future work

This thesis is framed in the context of the long-term goal of being able to determine experimentally O_2 diffusion in 3D cultures, specifically skin constructs. It was expected from the beginning that this project would focus on 2D cell cultures, as extensive experimentation was needed before reaching the point of taking measurements in 3D. Therefore, it is clear that there is ample room for future work in this context. But also within the scope of this project, there are limitations and aspects that could be improved. The main lines of work ahead and aspects of improvement are the following:

- Improvement in the fabrication protocol of the PtOEP membrane to obtain sensors with a more homogeneous response. The use of spin-coating could be studied.
- Further experimentation with 2D cell culture, possibly using a more accurate gas control system, to supplement conclusions of this work and to increase the working range of concentrations.
- Planning and development of experiments to measure O_2 diffusion dynamics in 3D tissues.
- Exploration of different platforms for the sensor, such as optical fiber sensors or nanoparticles.

6. SOCIO-ECONOMIC IMPACT, REGULATORY FRAMEWORK AND BUDGET

6.1. Socio-Economic Impact

Currently, technologies to fabricate artificial tissues, such as 3D bioprinting or tissue-on-a-chip technologies, are looking very promising and, therefore, are becoming an important target for investment. These technologies have two main applications: replacement of damaged tissues in patients and in-vitro drug testing.

Artificial organs and tissues, the possibility to engineer an organ from autologous cells from a patient, have the potential to revolutionize healthcare by solving the two main issues that organ transplants have nowadays: immunorejection and lack of availability of organ donations for every patient in need. Although the reality of having organs 'on demand', with the exception of skin, is still far away, research on this topic is attracting a lot of interest. Tissue-on-a-chip devices are mainly aimed at disease modelling and drug and cosmetic testing. Developing drugs is time consuming and expensive and these kinds of devices that are able to simulate multitissue interactions under near-physiological conditions provide very promising applications for pharmaceutical companies.

The impact that these technologies will have on healthcare, as well as economically, is unquantifiable. However, one of the key aspects necessary for the success of research on this field is a thorough understanding of the biological tissue to be replicated, not just the structure but also cell-cell interactions, what signaling molecules induce which functions or the different environmental cues that can affect physiological activity, among many others. It is true that technological advances are important, but one cannot replicate an organ without knowing what is happening or should happen at the biological level.

Within the general framework of deepening our understanding of different aspects of cell function, this work aims to study oxygen diffusion *in vitro*, focusing on skin cell culture. Wound care affects around 2% of the population of the US, accounting for a cost of $20 billion per year [45]. According to a UK report, treatment and care of chronic wounds accounts for 3% of the total cost of healthcare in developed countries [46]. In

future perspectives, being able to monitor oxygen concentration in cell culture systems will enhance our ability to build 3D culture systems under near physiological conditions, improving current state-of-the-art of wound care.

6.2. Regulatory Framework

The activities of this project were carried out in the *Bioengineering Laboratories* of *Universidad Carlos III de Madrid*. Actions in any laboratory must fulfil the standards and safety conditions established by the regulation. Prior to obtaining the authorization to work in the laboratory, a course on Occupational Risk Prevention was done, according to the regulations of the Biosafety Committee. According to the risks associated to the facilities, the work carried out for this thesis was developed in laboratories of biosafety levels 1 and 2 (BSL-1, BSL-2). At the regulatory level, all the work is under the regulation established by the Spanish government in RD 664/1997, on worker's protection against risks related to exposure to biological agents. It is also under European Union Law Council Directive 90/679/EEC of 26 November 1990.

The sensor at the center of this thesis is designed for research purpose, not intended as a device for commercialization nor to be used in a clinical environment for diagnosis or treatment. If it were the case, the product would need to be classified an comply with CE or FDA regulations.

6.3. Budget

This section includes detail of the main costs of the project. Tables 6.1 to 6.5 contain costs of sensor materials and reagents, cell culture reagents, laboratory consumables, equipment and personal costs, respectively. Subsequently, table 6.6 summarizes the total cost of the project. Only the main costs of the project have been calculated. The costs of using laboratory facilities, cleaning and very common laboratory equipment are not considered in this budget. With those considerations, the total estimated cost of the project is 16.229,82€. In table 6.7, the cost of fabrication of each membrane is calculated, including reagents and glass plates. The cost of a membrane in a round plate is 6.19€, the cost in a square well is 4.23€.

SENSOR MATERIALS AND REAGENTS

Product description	*Price (€) per unit*	*Amount used*	*Cost (€)*
PLATINUM OCTAETHYL-PORPHYRIN 95 % (100mg)	350,9	10mg	35,09
POLYSTYRENE, AVERAGE M.W. 280,000 (25g)	50,52	1g	2,0208
1,4-DIAZABICYCLO[2.2.2]OCTANE, REAGENTPL (25g)	24,32	0,24g	0,233472
Tetrahydrofuran reagent grade, =99.0%, c (1 L)	59,65	0,3L	17,90
BRAND Petri dish, glass (10 units)	22,63	20	45,25
8-well glass chamber (16u)	341,22	16	341,22
Sylgard 184 silicone elastomer kit (1,1kg)	198	0,1 kg	19,8
Collagen solution from bovine skin (20mL)	296,45	2mL	29,645
		Subtotal	491,15

Table 6.1. SENSOR MATERIALS AND REAGENTS

LABORATORY REAGENTS FOR CELL CULTURE

Product description	*Price (€) per unit*	*Amount used*	*Cost (€)*
DMEM (1X) + GlutaMAX (500mL)	27,1	2L	108,4
DMEM (1X) No Phenol Red	17,36	1L	17,36
FBS (500mL)	106,4	100mL	21,28
Antibiotic/Antimycotic Solution (100x) (20mL)	15,9	20mL	15,9
Trypsin (1X) (100mL)	12,75	50mL	6,38
alamarBlue™ Cell Viability Reagent (25mL)	321,86	3mL	38,62
		Subtotal	207,94

Table 6.2. LABORATORY REAGENTS FOR CELL CULTURE

EQUIPMENT & SOFTWARE

Product description	*Initial Cost (€)*	*Cost per year (€)*	*Period of use (months)*	*Cost (€)*
Leica DMi8	40000	8000	9	6000
Computer	700	140	9	105
MATLAB Student License	35	35	9	26,25
Microsoft Office	69	69	9	51,75
			Subtotal	6183

Table 6.3. EQUIPMENT & SOFTWARE

LABORATORY MATERIAL CONSUMABLES

Product description	*Price (€) per unit*	*Amount used*	*Cost (€)*
Small pipette tips (x1000)	19	1 pack	19
Medium pipette tips	19	1 pack	19
Large pipette tips	22	1 pack	22
Falcon tubes (15mL) (x500)	206,9	100	41,38
Falcon tubes (50mL) (x500)	209,33	100	41,87
Petri dish, polystyrene, p100 (x100)	106,8	70	74,76
PCR Plate, 96 well, skirted (x25)	120	3	14,4
0,45 um filter (x500)	1639	4	13,11
		Subtotal	245,52

Table 6.4. LABORATORY MATERIAL CONSUMABLES

PERSONNEL COSTS

Description	*Cost/hour (€)*	*Hours*	*Cost (€)*
Biomedical Engineer	15	300	4500
Project supervisor	70	45	3150
Laboratory technician	25	10	250
		Subtotal	7900

Table 6.5. PERSONNEL COSTS

COST SUMMARY	
Description	*Cost*
SENSOR MATERIALS AND REAGEANTS	491,15
LABORATORY REAGEANTS FOR CELL CULTURE	207,94
EQUIPMENT	6183
LABORATORY MATERIAL CONSUMABLES	245,52
PERSONNEL COSTS	7900
Subtotal	15027,61
Misc. (8%)	1202,21
TOTAL	**16229,82**

Table 6.6. COST SUMMARY

PRICE PER MEMBRANE

Concept	*Price (€) per unit*	*Price per mL membrane (€)*	*Round plate (€)*	*Square well (€)*
PLATINUM OCTAETHYLPORPHYRIN 95 % (100mg)	350,9	1,75	0,88	0,53
POLYSTYRENE, AVERAGE M.W. 280,000 (25g)	50,52	2,53	1,26	0,76
1,4-DIAZABICYCLO[2.2.2]OCTANE, REAGENTPL (25g)	24,32	0,01	0,01	0,00
Tetrahydrofuran reagent grade, =99.0%, c (1 L)	59,65	0,24	0,12	0,07
Sylgard 184 silicone elastomer kit (1,1kg)	198	-	0,18	0,06
Collagen solution from bovine skin (20mL)	296,45	-	1,48	0,15
BRAND Petri dish, glass (10 units)	22,625	-	2,26	-
8-well Chambered Coverglass w/ non-removable wells (16u)	341,22	-	-	2,67
		TOTAL	**6,19**	**4,23**

Table 6.7. PRICE PER MEMBRANE

BIBLIOGRAPHY

[1] K. Jungermann and T. Kietzmann, "Oxygen: Modulator of metabolic zonation and disease of the liver", *Hepatology*, vol. 31, no. 2, pp. 255–260, 2000.

[2] J. W. Allen and S. N. Bhatia, "Formation of steady-state oxygen gradients in vitro: Application to liver zonation", *Biotechnology and bioengineering*, vol. 82, no. 3, pp. 253–262, 2003.

[3] J. Malda, T. J. Klein, and Z. Upton, "The roles of hypoxia in the in vitro engineering of tissues", *Tissue engineering*, vol. 13, no. 9, pp. 2153–2162, 2007.

[4] C. M. Martín, *Tissue-on-a-chip design for skin modeling*, 2015.

[5] M. Carter and J. Shieh, *Chapter 14 - cell culture techniques*, ID: 312894, 2015 2015. DOI: https://doi.org/10.1016/B978-0-12-800511-8.00014-9.

[6] G. Invitrogen, "Cell culture basics", *Life technologies*, 2014.

[7] T. L. Riss *et al.*, "Cell viability assays", eng, in, G. S. Sittampalam *et al.*, Eds., ser. Assay Guidance Manual. Bethesda (MD), 2004. DOI: NBK144065[bookaccession].

[8] A. Mata, A. J. Fleischman, and S. Roy, "Characterization of polydimethylsiloxane (pdms) properties for biomedical micro/nanosystems", *Biomedical Microdevices*, vol. 7, no. 4, pp. 281–293, 2005.

[9] Y. J. Chuah *et al.*, "Simple surface engineering of polydimethylsiloxane with polydopamine for stabilized mesenchymal stem cell adhesion and multipotency", *Scientific reports*, vol. 5, p. 18 162, 2015.

[10] S. H. Tan, N.-T. Nguyen, Y. C. Chua, and T. G. Kang, "Oxygen plasma treatment for reducing hydrophobicity of a sealed polydimethylsiloxane microchannel", *Biomicrofluidics*, vol. 4, no. 3, p. 032 204, 2010.

[11] G. J. Tortora and B. Derrickson, *Principles of anatomy & physiology*. John Wiley & Sons, Incorporated, 2017.

[12] L. C. Junqueira and A. L. Mescher, *Junqueira's basic histology: text & atlas/Anthony L. Mescher*. New York [etc.]: McGraw-Hill Medical, 2013.

[13] C. Holzwarth *et al.*, “Low physiologic oxygen tensions reduce proliferation and differentiation of human multipotent mesenchymal stromal cells”, *BMC cell biology*, vol. 11, no. 1, p. 11, 2010.

[14] C. A. L. Bassett and I. Herrmann, “Influence of oxygen concentration and mechanical factors on differentiation of connective tissues in vitro”, *Nature*, vol. 190, no. 4774, p. 460, 1961.

[15] T. Kietzmann, “Metabolic zonation of the liver: The oxygen gradient revisited”, *Redox biology*, vol. 11, pp. 622–630, 2017.

[16] T. Kaufman and B. Hirshowitz, “The influence of various microclimate conditions on the burn wound: A review”, *Burns*, vol. 9, no. 2, pp. 84–88, 1982.

[17] J. P. Remensnyder and G. Majno, “Oxygen gradients in healing wounds”, eng, *The American journal of pathology*, vol. 52, no. 2, pp. 301–323, Feb. 1968, LR: 20181113; JID: 0370502; S88TT14065 (Oxygen); 1968/02/01 00:00 [pubmed]; 1968/02/01 00:01 [medline]; 1968/02/01 00:00 [entrez]; ppublish.

[18] E. A. O’Toole *et al.*, “Hypoxia increases human keratinocyte motility on connective tissue”, eng, *The Journal of clinical investigation*, vol. 100, no. 11, pp. 2881–2891, Dec. 1997, LR: 20181201; GR: P01 AR41045/AR/NIAMS NIH HHS/United States; GR: R01 AR33625/AR/NIAMS NIH HHS/United States; JID: 7802877; 0 (Blood Proteins); 0 (Cell Adhesion Molecules); 0 (Culture Media); 0 (Cytoskeletal Proteins); 0 (Integrins); 0 (Membrane Proteins); 0 (Microfilament Proteins); 0 (Phosphoproteins); 0 (Proteins); 0 (ezrin); 0 (kalinin); 144131-77-1 (moesin); 144517-21-5 (radixin); 9007-34-5 (Collagen); EC 2.7.10.1 (ErbB Receptors); EC 3.4.24.- (Collagenases); EC 3.4.24.35 (Matrix Metalloproteinase 9); S88TT14065 (Oxygen); 1998/02/12 00:00 [pubmed]; 1998/02/12 00:01 [medline]; 1998/02/12 00:00 [entrez]; ppublish. DOI: 10.1172/JCI119837[doi].

[19] K. R. Rivera *et al.*, “Integrated phosphorescence-based photonic biosensor (ipob) for monitoring oxygen levels in 3d cell culture systems”, *Biosensors and Bioelectronics*, vol. 123, pp. 131–140, 2019.

[20] C. Numako and I. Nakai, “Xafs studies of some precipitation and coloration reaction used in analytical chemistry”, *Physica B: Condensed Matter*, vol. 208, pp. 387–388, 1995.

[21] L. C. C. Jr, R. WOLF, D. GRANGER, and Z. TAYLOR, "Continuous recording of blood oxygen tensions by polarography", eng, *Journal of applied physiology*, vol. 6, no. 3, pp. 189–193, Sep. 1953, LR: 20181201; JID: 0376576; S88TT14065 (Oxygen); OID: CLML: 5425:17428:67:337:370; OTO: NLM; 1953/09/01 00:00 [pubmed]; 1953/09/01 00:01 [medline]; 1953/09/01 00:00 [entrez]; ppublish. DOI: 10.1152/jappl.1953.6.3.189[doi].

[22] L. Xiong and R. G. Compton, "Amperometric gas detection: A review", *Int.J.Electrochem.Sci*, vol. 9, pp. 7152–7181, 2014.

[23] *Clark electrode*. [Online]. Available: https://www.openanesthesia.org/aba%5C_clark%5C_electrode/.

[24] N. López-Ruiz *et al.*, *Determination of o2 using colour sensing from image processing with mobile devices*, ID: RS_609254005938ocessingwithmobiledevices, 2012. DOI: 10.1016/j.snb.2012.06.007.

[25] S.-K. Lee, M. Sheridan, and A. Mills, "Novel uv-activated colorimetric oxygen indicator", *Chemistry of Materials*, vol. 17, no. 10, pp. 2744–2751, 2005.

[26] S. M. Grist, L. Chrostowski, and K. C. Cheung, "Optical oxygen sensors for applications in microfluidic cell culture", *Sensors*, vol. 10, no. 10, pp. 9286–9316, 2010.

[27] X.-d. Wang, H.-x. Chen, Y. Zhao, X. Chen, and X.-r. Wang, "Optical oxygen sensors move towards colorimetric determination", *TrAC Trends in Analytical Chemistry*, vol. 29, no. 4, pp. 319–338, 2010.

[28] M. Ptaszek, "Rational design of fluorophores for in vivo applications", in, ser. Progress in molecular biology and translational science. Elsevier, 2013, vol. 113, pp. 59–108.

[29] M. Biesaga, K. Pyrzyńska, and M. Trojanowicz, "Porphyrins in analytical chemistry. a review", *Talanta*, vol. 51, no. 2, pp. 209–224, 2000.

[30] S. Nardis *et al.*, "Preparation and characterization of cobalt porphyrin modified tin dioxide films for sensor applications", *Sensors and Actuators B: Chemical*, vol. 103, no. 1-2, pp. 339–343, 2004.

[31] D. Delmarre and C. Bied-Charreton, "Grafting of cobalt porphyrins in sol–gel matrices: Application to the detection of amines", *Sensors and Actuators B: Chemical*, vol. 62, no. 2, pp. 136–142, 2000.

[32] X. Lu, I. Manners, and M. A. Winnik, "Polymer/silica composite films as luminescent oxygen sensors", *Macromolecules*, vol. 34, no. 6, pp. 1917–1927, 2001.

[33] S. R. Ricketts and P. Douglas, *A simple colorimetric luminescent oxygen sensor using a green led with pt octaethylporphyrin in ethyl cellulose as the oxygen-responsive element*, ID: 271353, Oct. 2008. DOI: https://doi.org/10.1016/j.snb.2008.07.017.

[34] P. Bhagwat, G. S. Achanta, D. Henthorn, and C.-S. Kim, "Colorimetric phosphorescence measurements with a color camera for oxygen determination", in *Smart Biomedical and Physiological Sensor Technology VIII*, vol. 8025, International Society for Optics and Photonics, 2011, 80250B.

[35] P. C. Thomas *et al.*, "A noninvasive thin film sensor for monitoring oxygen tension during in vitro cell culture", *Analytical Chemistry*, vol. 81, no. 22, pp. 9239–9246, 2009.

[36] F. Zeng, Z. Fan, S. Wu, X. Cheng, and Y. Tian, "Photo-patterned oxygen sensing films based on pt porphyrin for controlling cell growth and studying metabolism", *RSC Advances*, vol. 9, no. 2, pp. 924–930, 2019.

[37] C. Pulido and Ó. Esteban, *Tapered polymer optical fiber oxygen sensor based on fluorescence-quenching of an embedded fluorophore*, ID: 271353, 31 July 2013 2013. DOI: https://doi.org/10.1016/j.snb.2013.04.061.

[38] S. A. Vinogradov *et al.*, "Noninvasive imaging of the distribution in oxygen in tissue in vivo using near-infrared phosphors", *Biophysical journal*, vol. 70, no. 4, pp. 1609–1617, 1996.

[39] M. Sinaasappel and C. Ince, "Calibration of pd-porphyrin phosphorescence for oxygen concentration measurements in vivo", *Journal of applied physiology*, vol. 81, no. 5, pp. 2297–2303, 1996.

[40] R. J. Meier *et al.*, "Simultaneous photographing of oxygen and ph in vivo using sensor films", *Angewandte Chemie International Edition*, vol. 50, no. 46, pp. 10 893–10 896, 2011.

[41] B. Weyand *et al.*, "Noninvasive oxygen monitoring in three-dimensional tissue cultures under static and dynamic culture conditions", *BioResearch open access*, vol. 4, no. 1, pp. 266–277, 2015.

[42] H. Zirath *et al.*, “Every breath you take: Non-invasive real-time oxygen biosensing in two-and three-dimensional microfluidic cell models”, *Frontiers in physiology*, vol. 9, p. 815, 2018.

[43] *Invitrogen alamarblue assay manual*. [Online]. Available: http://tools.thermofisher.com/content/sfs/manuals/PI-DAL1025-1100_TI%20alamarBlue%20Rev%201.1.pdf.

[44] H. Bridle, “Optical detection technologies for waterborne pathogens”, in, ser. Waterborne Pathogens. Elsevier, 2014, pp. 119–145.

[45] R. G. Frykberg and J. Banks, “Challenges in the treatment of chronic wounds”, *Advances in wound care*, vol. 4, no. 9, pp. 560–582, 2015.

[46] K. Järbrink *et al.*, “The humanistic and economic burden of chronic wounds: A protocol for a systematic review”, *Systematic reviews*, vol. 6, no. 1, p. 15, 2017.